Response to Reviewer #1

(hess-2019-155)

Zhe Zhang, Yanping Li, Michael Barlage, Fei Chen, Gonzalo Miguez-Macho, Andrew Ireson, and Zhenhua Li

We appreciate the editor and two reviewers. They have put into time and effort to help us improve this article and their comments and suggestions are supportive and helpful. In the following text, the general response will be in red, original reviewers' comments and questions in black and our response to questions in blue.

In the REP simulation, we replaced the model default soil type, from a global 1-km resolution soil map, with the soil survey information, provided by the 11 groundwater well observations. This reviewer asked about how the REP approach change the conclusion on groundwater budget under future climate condition. As well in the comment 2, the reviewer asked about our culling criteria on selecting observation wells. The reviewer also provided us sources of groundwater wells and additional evaluation tools from GRACE satellite.

The first thing we address is to review the groundwater observation wells we selected in this study, as they provided critical information to evaluate our model output as well as soil properties to constrain our sensitivity study.

General Comments

This manuscript describes a land surface model linked to a basic groundwater model to investigate water table depth across the Prairie Pothole Region of North America. The coupled model is first used to represent recent conditions (2000 to 2013), then a future climate scenario. The manuscript addresses a relevant question regarding the hydrology of a large region and presents a method that would be applicable in other regions. The findings are interesting and would be of interest to researchers working in smaller areas within the Prairie Pothole Region. The approach demonstrates how cold region processes can be considered in large scale models that include a basic groundwater component

Specific Comments

There are 3 specific comments that warrant more attention:

1) One finding of the study is that simulated water table depth is sensitive to parameterization of the soil properties, which were input from a global dataset. The authors indicate that replacing some of the default soil type parameters with more location-specific information improves the match between simulated and observed water table depth (lines 448-453). This is great to see; however, there is no indication of the difference to the future climate scenario and water budget. The net effect on the primary question (i.e. future climate) is needed for completion. How much does the REP approach change the conclusions regarding distribution of recharge under the future climate? Addressing this issue would help the authors convey how important the fine-scale properties might be.

We appreciate that both reviewers have asked a question about the responses of REP soil under future PGW climate forcing (PGW forcing). This is also an important point we need better elaborate in the manuscript and in this reply.

We revisit the observational groundwater wells and select 33 out of 160 wells (see Answer 2) and replace the default soil with sand in these 33 locations. For the rest of the domain, we keep the default soil type from the 1-km global soil map. The complete list of 33 groundwater observation wells and the modeled WTD with default (DEF, blue lines) soil and REP soil (red lines) are in Fig. S4 at the end of this document. We also conducted a simulation with REP soil under PGW climate. Ten sites are presented here as they show diverse results in these sites (see Fig. S1).

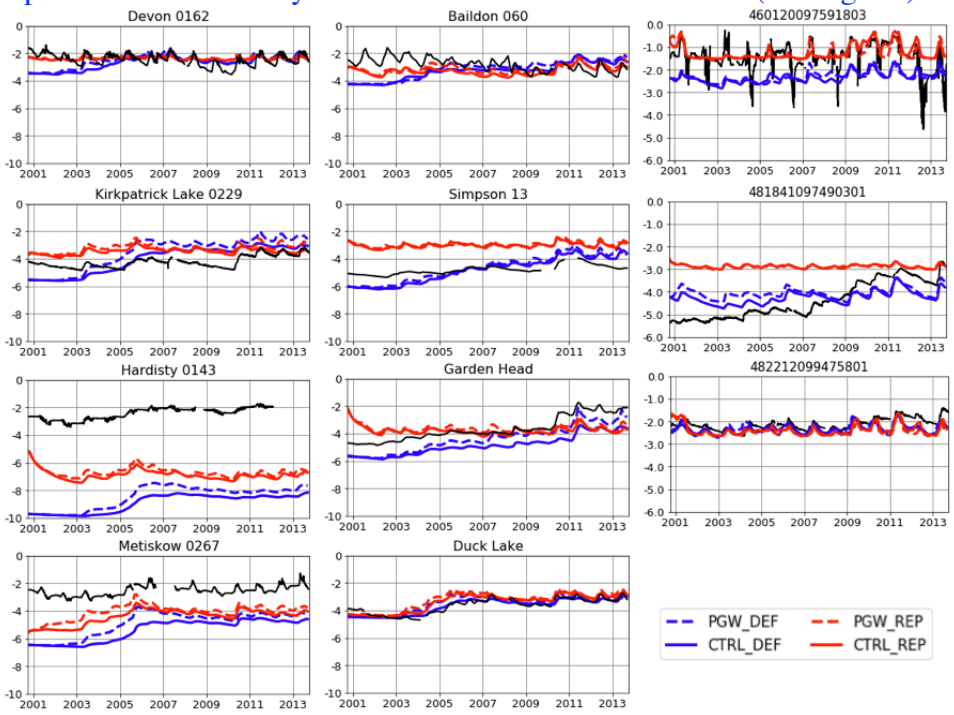

Fig. S1, the WTD dynamics of the observation and 4 model simulations: the two blue lines for default soil type (DEF), and two red lines for REP soil type (changed from default to sand); and solid lines for current climate (CTRL) and dashed line for future climate (PGW).

In general, under PGW climate, WTD rises due to increased precipitation and recharge. For some sites, the rise of WTD is more obvious in DEF soil rather than REP soil (e.g. Kirkpatrick Lake, Hardisty, Metiskow and 48184097490301). This is because the WTD under CTRL_REP is already higher than the WTD in CTRL_DEF and the Q_r term (groundwater discharge to rivers) is parameterized as the gradient between WTD and riverbed (Eq. (8)). As a loss term in the groundwater flux, Q_r is stronger in REP soil than in DEF soil and the climate change impacts on WTD rise is less prominent in REP soil than in DEF soil. On the other hand, there are some sites where PGW has little impacts on WTD, such as Simpson, Duck Lake and 482212099475801.

On point scale, given these diverse results over a limited number of sites, it is difficult to draw a universal conclusion but keep in mind the uncertainties and sensitivity of modeled WTD to soil parameters. On regional scale, the modifications of soil type at these 33 sites have little contribution to the large domain (401 x 396 grid points). Thus, our results of regional averaged water budget analysis in eastern and western PPR (Fig. 8 & 9) still hold. An ideal method to address this is to obtain sufficient information on soil properties accounting for horizontal and vertical heterogeneity. This is an on-going project that we are working on with the support from the Global Water Futures project. Future results and improvements can be expected.

2) The culling criteria for groundwater observation data may have been a bit ruthless. To end up with only 7% of the potential observation data seems quite aggressive. Whilst I don't disagree with the culling criteria, it would be helpful to have some additional points for spatial coverage that could be considered a "secondary" dataset (e.g. reported as supplemental material). To better understand (and accept) the culling procedure, some additional details are needed in lines 164-166. What is meant by a "sufficiently long record"? (provide an example or specify the timeframe). How were anthropogenic effects considered? Why was 7m selected as a cut off? Relaxing these criteria even just a little will increase the spatial coverage of your observation data.

Thank you for this comment and your concern about selecting observation wells. We have revisited the groundwater well observations and our selecting criteria in this revision. We use the daily water table depth records from total 160 groundwater wells in the domain, including 72 from the USGS, 43 from Alberta Environment and Parks, and 45 from Saskatchewan Water Security Agency. The locations of these 160 wells are shown in Fig. S2, together with the mean WTD and the availability of the observational records within the simulation period, respectively.

We revisited the criteria to select these groundwater wells: (1) the location of the well is close to the PPR region; (2) a sufficiently long record during the simulation period. We define the observation availability as the available observation period within the 13-year simulation period and select wells with observation availability greater than 80%; (3) unconfined aquifer with shallow groundwater (mean WTD > -5 m); and (4) has little anthropogenic influence (Fig. S3 shows an example of the impacts of pumping).

After these culling processes, 33 wells are selected, including 6 from Alberta, 13 from Saskatchewan, and 14 from the U.S. The locations of these 33 wells are shown in Fig. S2c and their information in Table S1. Table S2 also provides the statistics, including mean and standard deviation of WTD, for these 33 sites, from observation and our groundwater model. The complete timeseries of these 33 sites are shown at the end of this response.

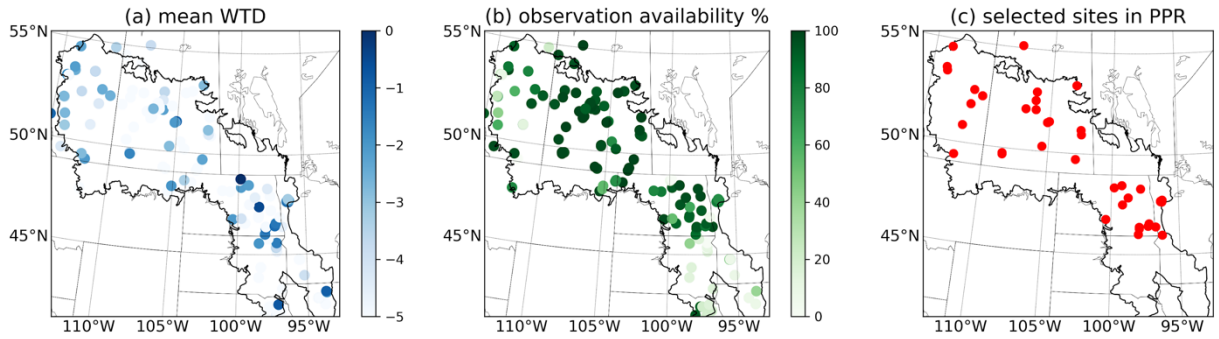

Fig. S2. The locations of the 160 groundwater wells in the PPR region and their (a) mean WTD values; (b) observation record availability; (c) the locations of 33 groundwater wells that have shallow groundwater level and long observation record (> 80%). A complete list of their information is presented in Table S1.

Table S1. Information about the selected 33 wells in the Prairie Pothole Region.

Site Name/ Site No.	Lat	Lon	Elevation	Aquifer type	Aquifer Lithology	Model Elevation	Model Soil type
Devon 0162	53.41	-113.76	700.0	Unconfined	Sand	697.366	Sandy loam
Hardisty 0143	52.67	-111.31	622.0	Unconfined	Gravel	633.079	Loam
Kirkpatrick Lake 0229	51.95	-111.44	744.5	Semi-confined	Sandstone	778.311	Sandy loam
Metiskow 0267	52.42	-110.60	677.5	Unconfined	Sand	679.516	Loamy sand
Wagner 0172	53.56	-113.82	670.0	Surficial	Sand	670.845	Silt loam
Narrow Lake 252	54.60	-113.63	640.0	Unconfined	Sand	701.0	Clay loam
Baildon 060	50.25	-105.50	590.184	Surficial	-	580.890	Sandy loam
Beauval	55.11	-107.74	434.3	Intertill	Sand	446.5	Sandy loam
Blucher	52.03	-106.20	521.061	Intertill	Sand/Gravel	523.217	Loam
Crater Lake	50.95	-102.46	524.158	Intertill	Sand/Gravel/Clay	522.767	Loam
Duck Lake	52.92	-106.23	502.920	Surficial	Sand	501.729	Loamy sand
Forget	49.70	-102.85	606.552	Surficial	Sand	605.915	Sandy loam
Garden Head	49.74	-108.52	899.160	Bedrock	Sand/Till	894.357	Clay loam
Nokomis	51.51	-105.06	516.267	Bedrock	Sand	511.767	Clay loam
Shaunavon	49.69	-108.50	896.040	Bedrock	Sand/Till	900.433	Clay loam
Simpson 13	51.45	-105.18	496.620	Surficial	Sand	493.313	Sandy loam
Simpson 14	51.457	-105.19	496.600	Surficial	Sand	493.313	Sandy loam
Yorkton 517	51.17	-102.50	513.643	Surficial	Sand/Gravel	511.181	Loam
Agrium 43	52.03	-107.01	500.229	Intertill	Sand	510.771	Loam
460120097591803	46.02	-97.98	401.177	Alluvial	Sand/Gravel	400.381	Sandy loam
461838097553402	46.31	-97.92	401.168	-	Sand/Gravel	404.719	Clay loam
462400097552502	46.39	-97.92	409.73	-	Sand/Gravel	407.405	Sandy loam
462633097163402	46.44	-97.27	325.52	Alluvial	Sand/Gravel	323.728	Sandy loam
463422097115602	46.57	-97.19	320.40	Alluvial	Sand/Gravel	314.167	Sandy loam
464540100222101	46.76	-100.37	524.91	-	Sand/Gravel	522.600	Clay loam
473841096153101	47.64	-96.25	351.77	Surficial	Sand/Gravel	344.180	Loamy sand
473945096202402	47.66	-96.34	327.78	Surficial	Sand/Gravel	328.129	Sandy loam
474135096203001	47.69	-96.34	325.97	Surficial	Sand/Gravel	327.764	Sandy loam
474436096140801	47.74	-96.23	341.90	Surficial	Sand/Gravel	336.210	Sandy loam
475224098443202	47.87	-98.74	451.33	-	Sand/Gravel	450.463	Sandy loam
481841097490301	48.31	-97.81	355.61	-	Sand/Gravel	359.568	Clay loam
482212099475801	48.37	-99.79	488.65	-	Sand/Gravel	488.022	Sandy loam
CRN Well WLN03	45.98	-95.20	410.7	Surficial	Sand/Gravel	411.4	Sandy loam

Table S2. Statistics of mean and standard deviation of WTD for the selected 33 wells in the Prairie Pothole Region. Bold texts indicate improvement in the REP than the CTRL run.

Site Name/Number	OBS_mean	CTRL_mean	REP_mean	OBS_std	CTRL_std	REP std
Devon 0162	-2.46	-2.69	**-2.38**	0.43	0.45	0.09
Hardisty 0143	-2.44	-8.91	**-6.88**	0.41	0.64	**0.36**
Kirkpatrick Lake 0229	-4.22	-4.03	-3.45	0.43	0.98	**0.22**
Metiskow 0267	-2.54	-5.39	**-4.43**	0.34	0.78	**0.55**
Narrow Lake 252	-2.31	-4.81	**-3.75**	0.28	0.60	0.51
Wagner 0172	-2.14	-8.06	**-2.70**	0.48	0.37	0.21
Baildon 060	-2.80	-3.29	**-3.20**	0.47	0.58	0.30
Beauval	-3.78	-4.85	**-4.20**	0.44	0.56	0.32
Blucher	-2.20	-4.24	**-2.16**	0.3	0.92	**0.26**
Crater Lake	-4.33	-3.97	-3.64	1.1	0.4	0.28
Duck Lake	-3.65	-3.69	-3.17	0.54	0.41	**0.62**
Forget	-2.28	-2.37	**-2.23**	0.33	0.17	0.19
Garden Head	-3.67	-4.85	**-3.77**	0.88	0.70	0.30
Nokomis	-1.04	-2.70	**-2.17**	0.23	0.55	**0.17**
Shaunavon	-1.62	-4.41	**-2.58**	0.42	0.69	0.20
Simpson 13	-4.82	-4.83	-3.02	0.31	0.91	**0.17**
Simpson 14	-2.03	-2.61	**-1.82**	0.34	0.18	**0.27**
Yorkton 517	-2.87	-3.97	**-1.98**	0.8	0.46	0.32
Agrium 43	-2.66	-3.75	**-3.38**	0.32	1.05	**0.36**
460120097591803	-1.44	-2.33	**-1.63**	0.56	0.24	**0.50**
461838097553402	-1.17	-2.32	**-1.68**	0.27	0.24	0.43
462400097552502	-4.9	-5.61	**-5.37**	0.29	0.09	**0.17**
462633097163402	-1.18	-1.49	**-1.02**	0.46	0.29	**0.54**
463422097115602	-1.36	-2.28	**-1.66**	0.34	0.23	0.49
464540100222101	-2.02	-3.64	**-2.78**	0.52	0.43	0.32
473841096153101	-0.77	-1.48	**-1.37**	0.24	0.18	0.51
473945096202402	-1.59	-1.58	-1.56	0.32	0.24	0.51
474135096203001	-0.72	-1.48	**-1.30**	0.33	0.25	0.54
474436096140801	-2.44	-2.29	-1.96	0.39	0.21	**0.40**
475224098443202	-4.52	-4.28	-5.31	0.75	0.52	0.34
481841097490301	-4.39	-4.24	-4.58	0.79	0.28	0.17
482212099475801	-2.13	-2.32	**-2.26**	0.24	0.20	0.17
CRN WLN 03	-2.04	-2.18	-1.88	0.24	0.18	0.43

Additionally, Fig. S2 provides an example of anthropogenic influence – pumping – which is the most common case in the PPR. The hydrograph is from a groundwater observation well in Vanscoy, SK (https://www.wsask.ca/Water-Info/Ground-Water/Observation-Wells/Vanscoy/) and the website has clear description about pumping from 2003 to 2007. The pumping impacts are not included in our model and we tend to study the impacts of climate to groundwater, therefore sites that have strong anthropogenic influences are removed from this study.

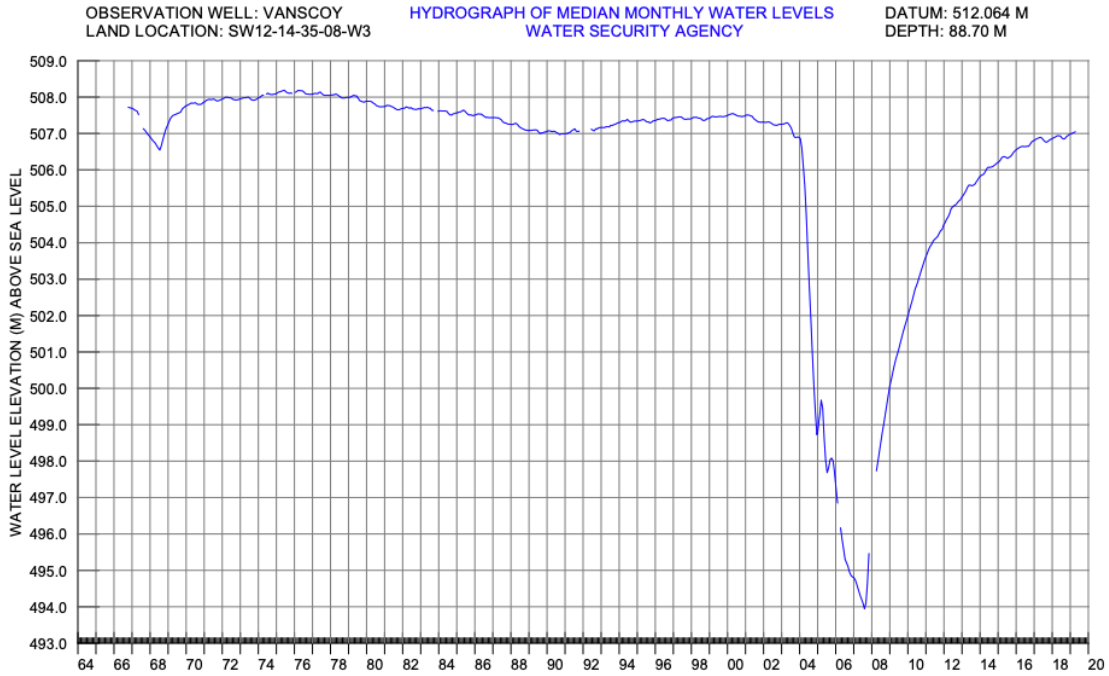

Fig. S3. An example of anthropogenic pumping on groundwater level in Vanscoy, SK. The pumping from 2003 to 2007 has a strong drawdown of water level about 13 m and the slow recovery takes almost 10 years returning to its normal level.

3) Related to the culling criteria, we evaluated the Alberta groundwater observation well data in a comparison with GRACE (Huang et al. 2016, Hydrogeology Journal v24, 1663-1680). You might be able to use Table 1 from that paper to increase the number of observation records. Also, you might be able to incorporate the GRACE comparison to water level data into your discussion and conclusions.

Thank you for your comment and this is a very useful suggestion. Whilst in Huang et al. 2016 the 36 sites are selected to evaluate the GRACE terrestrial water storage (TWS) anomaly rather than the water table depth (WTD) in this study. Therefore, the WTD anomaly or variation is the focus of Huang et al. 2016 and the records from these 36 sites have demonstrated a range of depth from shallow to deep, as well as from surficial and confined aquifer.

However, the groundwater model we used in this study is an unconfined shallow aquifer below 2-m soil layers, therefore we chose only to evaluate the wells with recorded WTD within 5 m below surface, which is also pointed out by other studies as the earth's critical zone where water table could have critical impacts to the land and above atmosphere. Thus, we cannot use several deep groundwater sites as in Huang's paper.

Technical Corrections

L17: Typo "on groundwater recharge rates"

Done.

L21: Is "mismatch" really the correct term? What you're describing is a parameter that is not represented in the model adequately. The resultant water table depth is mismatched, but the parameter is misrepresented.

Done. We remove this sentence from the abstract as there are multiple reasons of WTD mismatch. Thanks for the correction of "misrepresented parameters".

L23: Type "delaying the time. . ."

Done.

L47: A reference for the general concept of recharge and frozen soil would be useful (e.g. Hayashi)

Reference added (Niu and Yang 2006; Mohammed et al., 2018).

L61: Typo "discharge to rivers"

Done, thanks for the correction.

L64-65: Suggested edit ". . .snowmelt recharge to reach the water table, the previously upward water movement by capillary effect to reverse and move downwards, and allow the water table to rise to. . ."

Done. Thank you for the suggestion.

L66: Suggest removing "and desiccates the soil", as this starts to invoke ideas of seasonally varying parameters.

Done.

L76: Provide a reference for the 5-40mm/yr example.

Thanks. Reference (Hayashi et al., 2016) is added and the paragraph is moved to discussion.

L80: Typo ". . .this is challenging to represent in current. . ."

Done, thank you for the correction.

L85: Typo "suggested"

Done.

L97: Typo "groundwater models"

Done.

L128: What is meant by "groundwater evolution"? Do you simply mean water table dynamics?

Yes, thanks for the correction.

L143: Typo ". . .from the WRF. . ."

Thanks for the correction.

L148: You might want to mention that most of the observation well data will be biased toward more permeable deposits (e.g. sand and gravel). Typically, provincial and state agencies don't monitor low permeability formation.

Thank you for this information. Very helpful to include this in this paper.

L153: Alberta Environment and Parks

Done.

L164: Provide an example timeframe

Fig. S1b provides the observation availability of the groundwater wells within the 13-year simulation period.

L165: How was anthropogenic effect determined?

The anthropogenic effects were determined by the site description on the Saskatchewan Water Security Agency websites. An example of anthropogenic pumping is provided in Fig. S2.

L259: Add "in the PPR" to the end of this sentence
Done.
L285-288: The model initialization process is unclear. Spin up times of 500 years and 4 years are mentioned here. Is the 4 yr period simply to account for grid size difference, and essentially following the 500 yr spin up in the previous model?
Thank you for this quesiton. The 500-year spin-up uses a 30-year climatology recharge as upper boundary condition. And the 4-year spin-up uses the forcing from 2000 Oct to 2001 Sep, and runs this year continuesouly for 4 loops, accounting for grid size difference and a more realistic initial condition at the beginning of the simulation. In this revision, we have the opportunity to do a longer spin-up for 10-year loop.
L317-318: Relation to Amazon with is not relevant and totally looks like self-citation here. The concept of infiltration response is pretty basic.
Thank you for this comment. The Amazon study reference (Miguez-Macho et al., 2012) is a study applying the same groundwater model in Amazon rainforest, in which similar shortcomings are reported as in our study. Thus, we believe this is a relevant study of modeling water table depth using MMF groundwater scheme.
L321: By "out-of-the-box" do you simply mean "uncalibrated"?
Yes.
L323: Instead of "further study" do you mean "preliminary study", because later in the manuscript modified parameters are used (i.e. REP) Section 3.2 and 3.3: A little bit of set-up is needed here. Are the results presented averages over a certain period? What timeframe for the water budget components correspond to? (3 months)
Thanks for the quesiton. "Further study" refers to the later-on analysis of groundwater fluxes and water balance in section 3.2 and 3.3. The results presented averages over a monthly interval.
L425: Typo ". . .in the locations of the observations well."
Done.
L448-453: This section kinda teases the reader. How do the future scenario results look with the REP parameters?
Thanks for the question. We appreciate this question and please see Answer 1 for detailed response.
L520: Typo "As a result. . ."
Thanks for the correction.

Reference

Hayashi, M., van der Kamp, G. and Rosenberry, D. O.: Hydrology of Prairie Wetlands: Understanding the Integrated Surface-Water and Groundwater Processes, Wetlands, 36, 237–254, doi:10.1007/s13157-016-0797-9, 2016.

Koren, V., Schaake, J., Mitchell, K., Duan, Q.-Y., Chen, F. and Baker, J. M.: A parameterization of snowpack and frozen ground intended for NCEP weather and climate models, J. Geophys. Res. Atmos., 104(D16), 19569–19585, doi:10.1029/1999JD900232, 1999.

Mohammed, A. A., Kurylyk, B. L., Cey, E. E. and Hayashi, M.: Snowmelt Infiltration and Macropore Flow in Frozen Soils: Overview, Knowledge Gaps, and a Conceptual Framework, Vadose Zo. J., 17(1), doi:10.2136/vzj2018.04.0084, 2018.

Niu, G.-Y. and Yang, Z.-L.: Effects of Frozen Soil on Snowmelt Runoff and Soil Water Storage at a Continental Scale, J. Hydrometeorol., 7(5), 937–952, doi:10.1175/JHM538.1, 2006.

Response to Reviewer #2

(hess-2019-155)

Zhe Zhang, Yanping Li, Michael Barlage, Fei Chen, Gonzalo Miguez-Macho, Andrew Ireson, and Zhenhua Li

Zhang et al. use a land surface model coupled to a two-way groundwater dynamics model to explore the response of groundwater to climate change in the Prairie Pothole Region (PPR) of North America. The main research objectives of this study were to simulate two-way exchange in the subsurface, characterize groundwater response to climate change, and identify the major processes controlling this response in the region. The novel methodological components of this study include the application of a two-way groundwater exchange module coupled to a land surface model and the use of regional scale WRF CONUS model outputs with a scheme that treats convective precipitation. The authors point out that there is a need to explore hydrologic response to climate change at the regional scale, of which there is currently a gap, and so this study is a timely and important addition to that area of research.

We appreciate the editor and two reviewers. They have put into time and effort to help us improve this article and their comments and suggestions are supportive and helpful. In the following text, the general response will be in red, original reviewers' comments and questions in black and our answers to the questions in blue.

My main comments are:

1. The authors need to introduce their research objective earlier in the introduction, and better organize the following paragraphs around the background and motivation for the study. In particular, I would like to see more motivation for the methodological set up of the study. For example, if prairie pothole hydrogeology is so complex at the local scale (lines 70-83), why is a coarse regional model appropriate? Second, since the freeze thaw process is a key requirement for PPR hydrogeology, I would like to see more background (including references) of how this process has been treated in various LSMs and also more information in the methods section of how NOAH-MP represents it.

Thank you for the comment. This comment is very good and contains several questions. We would break this down and answer it separately.

The order of the paragraphs has been reorganized in the manuscript. The objectives of this study have been moved ahead in Introduction. The prairie pothole wetlands and groundwater-wetland exchanges is now moved to Discussion. More details for the methodological set-up, such as frozen soil treatments in LSMs, have been added in Data and Methods.

We move L70-83 to the Discussion section. This paragraph in the original manuscript introduced important ecosystem services provided by prairie pothole wetlands and the interactions between groundwater flow and these wetlands. Fine-scale processes (usually from 10 to 100 m), such as snow drift, runoff fill-spill and groundwater recharge/discharge to wetlands, have complicated the water balance in these wetlands and are challenging to LSMs (usually from 1 to 100 km) (Hayashi et al). In this work, we configured our model domain at 4-km resolution, and we acknowledged that it is insufficient to resolve these fine-scale processes. This is a current limit and future

challenge in this study area. We are currently developing sub-grid parameterization scheme to represent the presence of these fine-scale prairie pothole wetlands to the hydrological cycle, including ET and sub-surface flows. Please see the Discussion section for more details.

We add a paragraph in Introduction to provide background of frozen soil parameterizations in most common LSMs, such as CLM, NoahV3, and Noah-MP. Additionally, a description of Noah-MP frozen soil parameterizations is included in the Methods section. There are two options in Noah-MP for frozen soil permeability; option 1 is the default option in Noah-MP LSM and is adapted from Niu and Yang (2006); option 2 is inherited the Koren et al. (1999) scheme from NoahV3. We used the option 1 in our simulation. The option 1 assumes that a model grid cell consists of permeable and impermeable areas and thus uses the total soil moisture to compute hydraulic properties of the soil. The option 2 uses only the liquid water volume to calculate hydraulic properties. Additionally, option 1 assumes that soil ice has a linear (smaller) effect on infiltration, generally simulates more permeable frozen soil than option 2, which assumes soil ice has a non-linear (greater) effect on soil permeability (Niu et al., 2011). For this reason, the option 1 allows the soil water to move and redistribute more easily within the frozen soil.

2. More information is needed on the criteria for selecting wells, such as required length of record and how anthropogenic effects were minimized. Further, comparing a coarse land surface model covering a large total area (the model area is not reported) to only 11 wells is concerning. From Fig. 1 it appears that quite a large portion of the PPR does not have any well coverage. I think it would be worth revisiting the criteria and including a few more wells out of the 160. If that's not possible, then more discussion regarding potential uncertainty in capturing groundwater dynamics in PPR sub-regions without wells (e.g. the southwest portion) is warranted.

Thank you for this comment and your concern about selecting observation wells. We have revisited the groundwater well observations and our selecting criteria in this revision. We use the daily water table depth records from total 160 groundwater wells in the domain, including 72 from the USGS, 43 from Alberta Environment and Parks, and 45 from Saskatchewan Water Security Agency. The locations of these 446 wells are shown in Fig. S1, together with the mean WTD and the availability of the observational records within the simulation period, respectively. (The model domain contains 401 x 396 grid points and is added in the Methods section).

We revisited the criteria to select these groundwater wells: (1) the location of the well is close to the PPR region; (2) a sufficiently long record during the simulation period. We define the observation availability as the available observation period within the 13-year simulation period and select wells with observation availability greater than 80%; (3) unconfined aquifer with shallow groundwater (mean WTD > -5 m); and (4) has little anthropogenic influence.

After these culling processes, 33 wells are selected, including 6 from Alberta, 13 from Saskatchewan, and 14 from the U.S., and the locations of these 33 wells are shown in Fig. S1c and their information in Table S1. Table S2 also provides the statistics, including mean and standard deviation of WTD, for these 33 sites, from observation and our groundwater model. The complete timeseries of these 33 sites are shown at the end of this response.

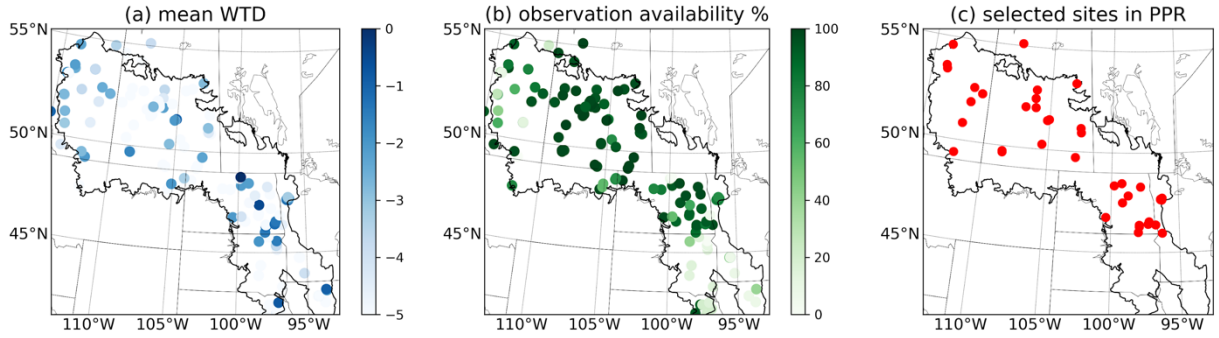

Fig. S1. The locations of the 160 groundwater wells in the PPR region and their (a) mean WTD values; (b) observation record availability; (c) the locations of 33 groundwater wells that have shallow groundwater level and long observation record (> 80%). A complete list of their information is presented in Table S1.

Table S1. Information about the selected 33 wells in the Prairie Pothole Region.

Site Name/ Site No.	Lat	Lon	Elevation	Aquifer type	Aquifer Lithology	Model Elevation	Model Soil type
Devon 0162	53.41	-113.76	700.0	Unconfined	Sand	697.366	Sandy loam
Hardisty 0143	52.67	-111.31	622.0	Unconfined	Gravel	633.079	Loam
Kirkpatrick Lake 0229	51.95	-111.44	744.5	Semi-confined	Sandstone	778.311	Sandy loam
Metiskow 0267	52.42	-110.60	677.5	Unconfined	Sand	679.516	Loamy sand
Wagner 0172	53.56	-113.82	670.0	Surficial	Sand	670.845	Silt loam
Narrow Lake 252	54.60	-113.63	640.0	Unconfined	Sand	701.0	Clay loam
Baildon 060	50.25	-105.50	590.184	Surficial	-	580.890	Sandy loam
Beauval	55.11	-107.74	434.3	Intertill	Sand	446.5	Sandy loam
Blucher	52.03	-106.20	521.061	Intertill	Sand/Gravel	523.217	Loam
Crater Lake	50.95	-102.46	524.158	Intertill	Sand/Gravel/Clay	522.767	Loam
Duck Lake	52.92	-106.23	502.920	Surficial	Sand	501.729	Loamy sand
Forget	49.70	-102.85	606.552	Surficial	Sand	605.915	Sandy loam
Garden Head	49.74	-108.52	899.160	Bedrock	Sand/Till	894.357	Clay loam
Nokomis	51.51	-105.06	516.267	Bedrock	Sand	511.767	Clay loam
Shaunavon	49.69	-108.50	896.040	Bedrock	Sand/Till	900.433	Clay loam
Simpson 13	51.45	-105.18	496.620	Surficial	Sand	493.313	Sandy loam
Simpson 14	51.457	-105.19	496.600	Surficial	Sand	493.313	Sandy loam
Yorkton 517	51.17	-102.50	513.643	Surficial	Sand/Gravel	511.181	Loam
Agrium 43	52.03	-107.01	500.229	Intertill	Sand	510.771	Loam
460120097591803	46.02	-97.98	401.177	Alluvial	Sand/Gravel	400.381	Sandy loam
461838097553402	46.31	-97.92	401.168	-	Sand/Gravel	404.719	Clay loam
462400097552502	46.39	-97.92	409.73	-	Sand/Gravel	407.405	Sandy loam
462633097163402	46.44	-97.27	325.52	Alluvial	Sand/Gravel	323.728	Sandy loam
463422097115602	46.57	-97.19	320.40	Alluvial	Sand/Gravel	314.167	Sandy loam
464540100222101	46.76	-100.37	524.91	-	Sand/Gravel	522.600	Clay loam
473841096153101	47.64	-96.25	351.77	Surficial	Sand/Gravel	344.180	Loamy sand
473945096202402	47.66	-96.34	327.78	Surficial	Sand/Gravel	328.129	Sandy loam
474135096203001	47.69	-96.34	325.97	Surficial	Sand/Gravel	327.764	Sandy loam
474436096140801	47.74	-96.23	341.90	Surficial	Sand/Gravel	336.210	Sandy loam
475224098443202	47.87	-98.74	451.33	-	Sand/Gravel	450.463	Sandy loam
481841097490301	48.31	-97.81	355.61	-	Sand/Gravel	359.568	Clay loam
482212099475801	48.37	-99.79	488.65	-	Sand/Gravel	488.022	Sandy loam
CRN Well WLN03	45.98	-95.20	410.7	Surficial	Sand/Gravel	411.4	Sandy loam

Table S2. Statistics of mean and standard deviation of WTD for the selected 33 wells in the Prairie Pothole Region. Bold number indicates the REP run has improved results than the CTRL run.

Site Name/Number	OBS_mean	CTRL_mean	REP_mean	OBS_std	CTRL_std	REP std
Devon 0162	-2.46	-2.69	**-2.38**	0.43	0.45	0.09
Hardisty 0143	-2.44	-8.91	**-6.88**	0.41	0.64	**0.36**
Kirkpatrick Lake 0229	-4.22	-4.03	-3.45	0.43	0.98	**0.22**
Metiskow 0267	-2.54	-5.39	**-4.43**	0.34	0.78	**0.55**
Narrow Lake 252	-2.31	-4.81	**-3.75**	0.28	0.60	0.51
Wagner 0172	-2.14	-8.06	**-2.70**	0.48	0.37	0.21
Baildon 060	-2.80	-3.29	**-3.20**	0.47	0.58	0.30
Beauval	-3.78	-4.85	**-4.20**	0.44	0.56	0.32
Blucher	-2.20	-4.24	**-2.16**	0.3	0.92	**0.26**
Crater Lake	-4.33	-3.97	-3.64	1.1	0.4	0.28
Duck Lake	-3.65	-3.69	-3.17	0.54	0.41	**0.62**
Forget	-2.28	-2.37	**-2.23**	0.33	0.17	0.19
Garden Head	-3.67	-4.85	**-3.77**	0.88	0.70	0.30
Nokomis	-1.04	-2.70	**-2.17**	0.23	0.55	**0.17**
Shaunavon	-1.62	-4.41	**-2.58**	0.42	0.69	0.20
Simpson 13	-4.82	-4.83	-3.02	0.31	0.91	**0.17**
Simpson 14	-2.03	-2.61	**-1.82**	0.34	0.18	**0.27**
Yorkton 517	-2.87	-3.97	**-1.98**	0.8	0.46	0.32
Agrium 43	-2.66	-3.75	**-3.38**	0.32	1.05	**0.36**
460120097591803	-1.44	-2.33	**-1.63**	0.56	0.24	**0.50**
461838097553402	-1.17	-2.32	**-1.68**	0.27	0.24	0.43
462400097552502	-4.9	-5.61	**-5.37**	0.29	0.09	**0.17**
462633097163402	-1.18	-1.49	**-1.02**	0.46	0.29	**0.54**
463422097115602	-1.36	-2.28	**-1.66**	0.34	0.23	0.49
464540100222101	-2.02	-3.64	**-2.78**	0.52	0.43	0.32
473841096153101	-0.77	-1.48	**-1.37**	0.24	0.18	0.51
473945096202402	-1.59	-1.58	-1.56	0.32	0.24	0.51
474135096203001	-0.72	-1.48	**-1.30**	0.33	0.25	0.54
474436096140801	-2.44	-2.29	-1.96	0.39	0.21	**0.40**
475224098443202	-4.52	-4.28	-5.31	0.75	0.52	0.34
481841097490301	-4.39	-4.24	-4.58	0.79	0.28	0.17
482212099475801	-2.13	-2.32	**-2.26**	0.24	0.20	0.17
CRN WLN 03	-2.04	-2.18	-1.88	0.24	0.18	0.43

3. More information is needed on the climate change scenarios such as what emissions scenario was used and what sort of temperature increase does that roughly translate to?

Thank you for this comment, we have added the information about emission scenario for the PGW forcing. The climate change forcing used in this LSM study is from a regional convective-permitting modeling project in North America, called WRF CONUS. Liu et al. (2017) discussed the WRF CONUS project in details. The CTRL run is forced with 6-hour ERA-Interim data, representing the current climate. The PGW run is forced with the ERA-Interim data plus a climate perturbation derived from CMIP5 ensemble under the RCP8.5 emission scenario, representing the future climate change till the end of 21st century. Fig. 4 and 5 in the manuscript show the temperature and precipitation change in PGW-CTRL. The most significant warming occurs in the winter over northern region and mountainous region in Alberta, warming up to 8 °C. An overall increase in precipitation is shown in Fig. 5, except in summer in the southeast, about 50 to 100 mm reduction.

4. If the REP model performed better against observational data, then why didn't the authors choose to run the climate change scenario using that parameterization? Including such a simulation would give the reader a sense of how sensitive projections are to model parameterization. If including this simulation is too computationally expensive, then at least some discussion of how the climate projections might be sensitive to.

We appreciate that both reviewers have asked a question about the responses of REP soil under future PGW climate forcing (PGW forcing). This is also an important point we need better elaborate in the manuscript and in this reply.

We revisit the observational groundwater wells and select 33 out of 160 wells (see Answer 2) and replace the default soil with sand in these 33 locations. For the rest of the domain, we keep the default soil type from the 1-km global soil map. The complete list of 33 groundwater observation wells and the modeled WTD with default (DEF, blue lines) soil and REP soil (red lines) are in Fig. S3 at the end of this document. We also conducted a simulation with REP soil under PGW climate. Ten sites are presented here as they show diverse results in these sites (see Fig. S2).

In general, under PGW climate, WTD rises due to increased precipitation and recharge. For some sites, the rise of WTD is more obvious in DEF soil rather than REP soil (e.g. Kirkpatrick Lake, Hardisty, Metiskow and 48184097490301). This is because the WTD under CTRL_REP is already higher than the WTD in CTRL_DEF and the Q_r term (groundwater discharge to rivers) is parameterized as the gradient between WTD and riverbed (Eq. (8)). As a loss term in the groundwater flux, Q_r is stronger in REP soil than in DEF soil and the climate change impacts on WTD rise is less prominent in REP soil than in DEF soil. On the other hand, there are some sites where PGW has little impacts on WTD, such as Simpson, Duck Lake and 482212099475801.

On point scale, given these diverse results over a limited number of sites, it is difficult to draw a universal conclusion but keep in mind the uncertainties and sensitivity of modeled WTD to soil parameters. On regional scale, the modifications of soil type at these 33 sites have little contribution to the large domain (401 x 396 grid points). Thus, our results of regional averaged water budget analysis in eastern and western PPR (Fig. 8 & 9) still hold. An ideal method to address this is to obtain sufficient information on soil properties accounting for horizontal and vertical

heterogeneity. This is an on-going project that we are working on with the support from the Global Water Futures project and future improvements can be expected.

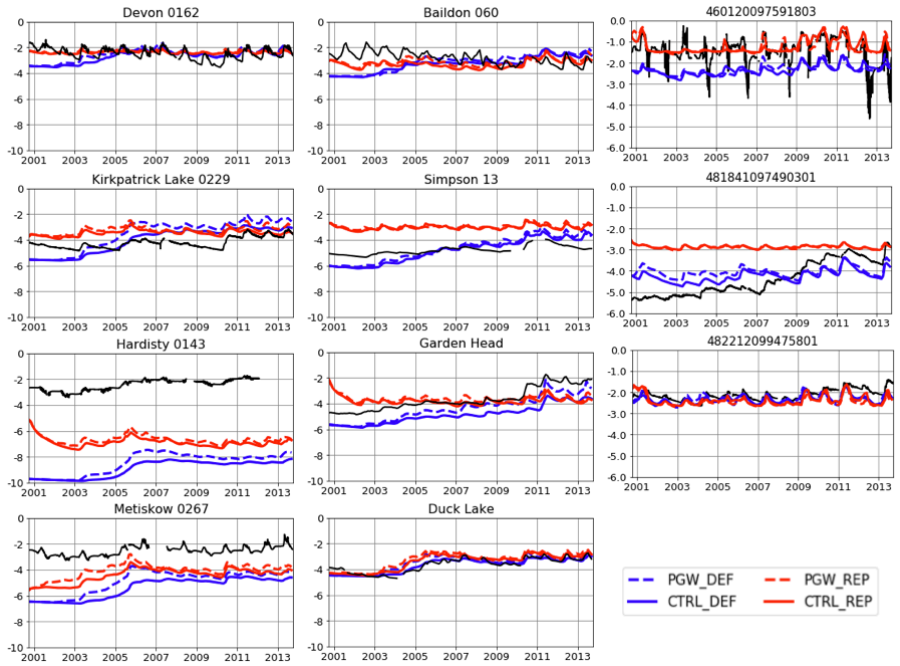

Fig. S2, the WTD dynamics of the observation and 4 model simulations: the two blue lines for default soil type (DEF), and two red lines for REP soil type (changed from default to sand); and solid lines for current climate (CTRL) and dashed line for future climate (PGW).

5. There is a fairly major typographical error in the text and figure captions. Delta S should be equal to R + Qlat – Qr (according to equation 4), but it is repeatedly written as R + Qlat + Qr (equation 10, for example) in the paper. This is hopefully only typographical, as that would result in large errors in reported changes in storage.

Thank you very much for pointing out this typo mistake. The *Qr* term characterizes the groundwater discharge to maintain river flow and in the model this term is always positive, meaning water flow from aquifer to riverbed. This is a loss term to the groundwater aquifer and that's why there is a negative sign before the term. I have corrected this in the manuscript, please see.

6. The figure captions in the text often do not match the figure captions associated with the figures. Further, the authors should write out fully descriptive figure captions, including defining acronyms, such that the figures would be able to be read on their own. There are currently several figure captions that simply says, "same as Fig. xx."
Thank you for the comment. Figure captions have been changed.

7. Finally, the timing and amount of thaw is a key control on recharge projections, but the authors do not explore or discuss how well their model captures freeze-thaw dynamics at the regional scale. This is related to my earlier comment, that the authors need to explain how this process is represented in their model. Some discussion of how future studies could improve upon this methodology to capture this important and heterogeneous process would also add strength to the paper.

Thank you very much and we appreciate this comment. In this revision, we introduced the frozen soil parameterizations in Noah-MP and other LSMs in the Introduction and Methods section. Although it is still a challenge to explore freeze-thaw dynamics on regional scale, we include some discussion on this matter and hope it can encourage future studies.

To our knowledge, there is no direct observation of soil ice for large region coverage. Most of the existing soil ice measurement are on local scale, for example, measurement from the FLUXNET sites, and have been used in for model evaluation (Niu and Yang 2006; Niu et al., 2011). Yang et al. (2011) provided a regional analysis on runoff, using the University of New Hampshire-Global Runoff Data Center dataset, and inferred the improved runoff simulation is the more permeable frozen soil in Noah-MP. These contents are also added to the Discussion as well.

Specific comments:
There were quite a number of typographical errors, a few of which I will list here, but I do recommend the authors go back over the manuscript with a closer eye for spelling and grammatical errors.

Line 55: use a different acronym for precipitation- PR is too close to PPR
Lines 64-65: rewrite for grammar
Thanks for the correction, done.

Line 76: provide citation for recharge estimate
Thanks for the correction, reference (Hayashi et al., 2016) added.

Line 77: rewrite for grammar
Line 80: rewrite for grammar
Done. This paragraph is now moved to Discussion.

Lines 93-94: studies of regional climate change impacts to hydrology in N. America: Niraula et al., 2017a,b, Christensen et al., 2004
Thanks for these citations, added in the reference list.

Line 148: Observational data
Line 181: define offline mode
Lines 341 and 350: under current/future climate conditions
Thank you for the correction.

Line 372: what is Qdrain?
Should be "negative recharge". Corrected in the manuscript.

Line 474: include citation
Thank you for the reminder. Reference (Pokhrel et al., 2014) added in the list.

Lines 520-522: rewrite for grammar
Done.

Table 1: either use descriptive column names or define any abbreviation used. Add units where needed.
Thank you, definitions of abbreviation are added.

Reference

Hayashi, M., van der Kamp, G. and Rosenberry, D. O.: Hydrology of Prairie Wetlands: Understanding the Integrated Surface-Water and Groundwater Processes, Wetlands, 36, 237–254, doi:10.1007/s13157-016-0797-9, 2016.

Koren, V., Schaake, J., Mitchell, K., Duan, Q.-Y., Chen, F. and Baker, J. M.: A parameterization of snowpack and frozen ground intended for NCEP weather and climate models, J. Geophys. Res. Atmos., 104(D16), 19569–19585, doi:10.1029/1999JD900232, 1999.

Mohammed, A. A., Kurylyk, B. L., Cey, E. E. and Hayashi, M.: Snowmelt Infiltration and Macropore Flow in Frozen Soils: Overview, Knowledge Gaps, and a Conceptual Framework, Vadose Zo. J., 17(1), doi:10.2136/vzj2018.04.0084, 2018.

Niu, G.-Y. and Yang, Z.-L.: Effects of Frozen Soil on Snowmelt Runoff and Soil Water Storage at a Continental Scale, J. Hydrometeorol., 7(5), 937–952, doi:10.1175/JHM538.1, 2006.

Pokhrel, Y. N., Fan, Y. and Miguez-Macho, G.: Potential hydrologic changes in the Amazon by the end of the 21st century and the groundwater buffer, Environ. Res. Lett., 9(8), doi:10.1088/1748-9326/9/8/084004, 2014.

Supplemental Materials - WTD dynamics from 33 groundwater wells in the PPR

Alberta Environment and Parks

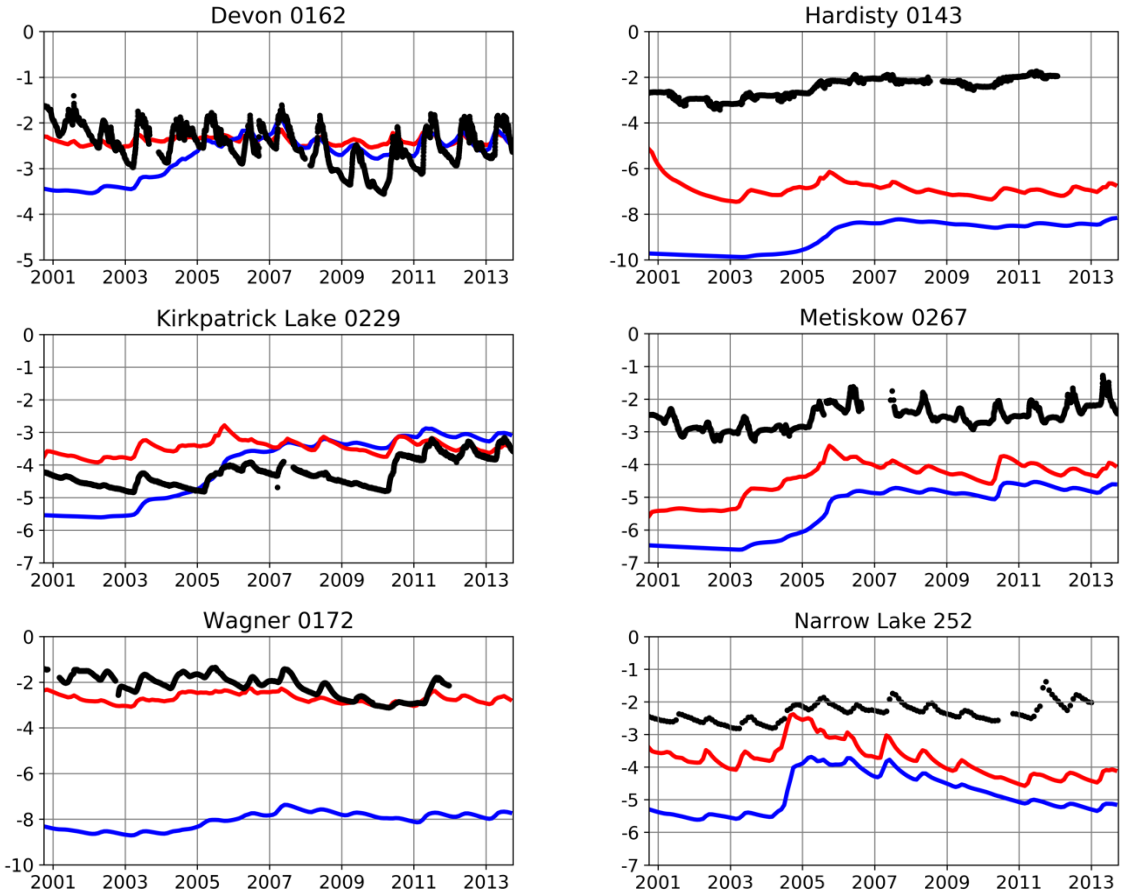

Saskatchewan Water Securtiy Agency

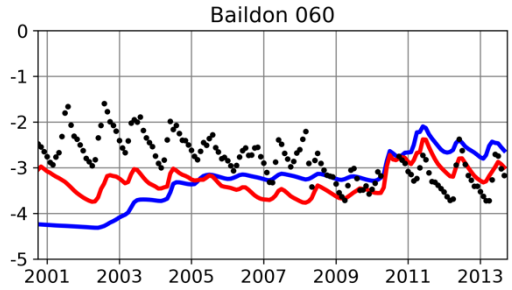

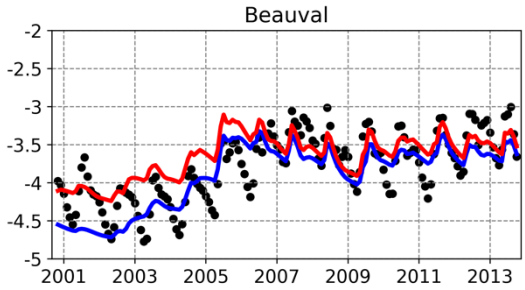

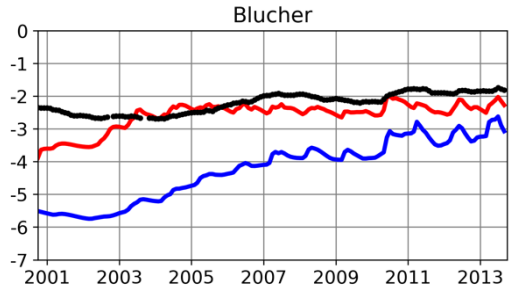

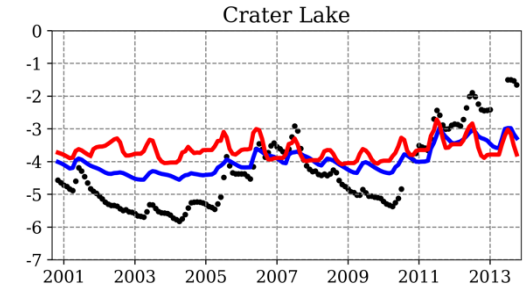

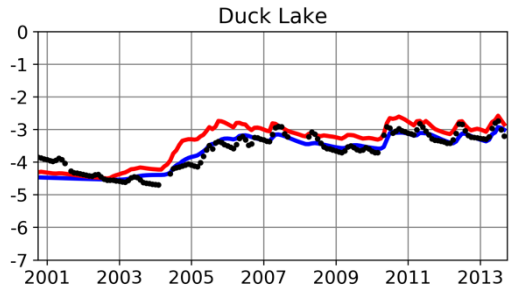

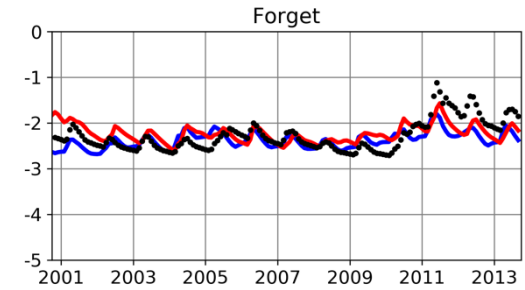

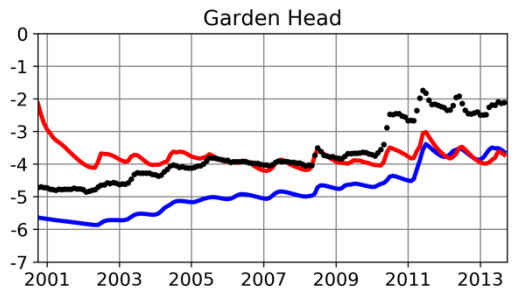

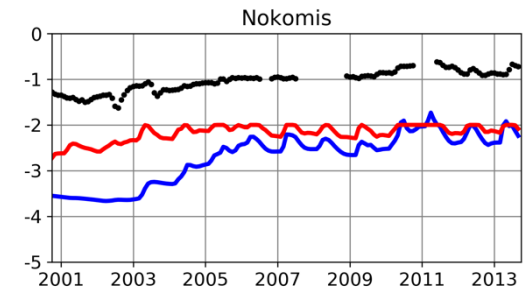

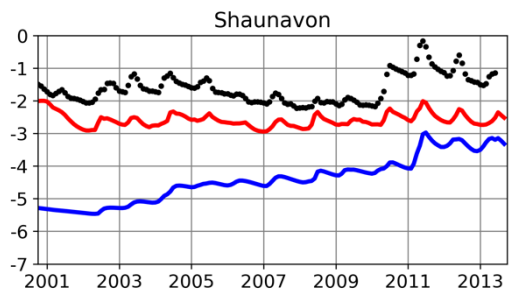

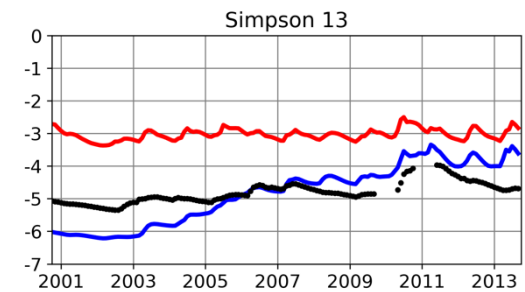

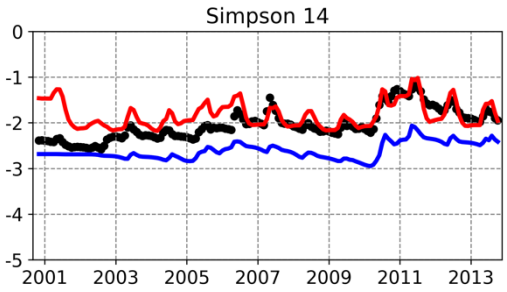
Simpson 14
0
-1
-2
-3
-4
-5
2001
2003
2005
2007
2009
2011
2013

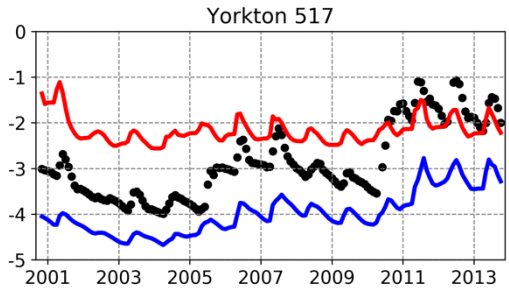
Yorkton 517
0
-1
-2
-3
-4
-5
2001
2003
2005
2007
2009
2011
2013

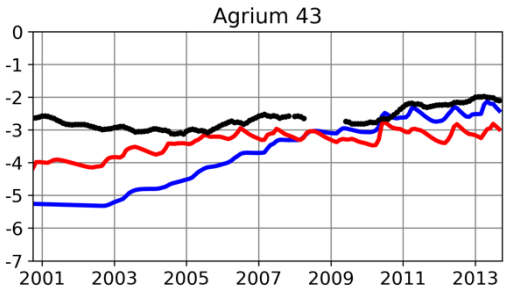
Agrium 43
0
-1
-2
-3
-4
-5
-6
-7
2001
2003
2005
2007
2009
2011
2013

USGS

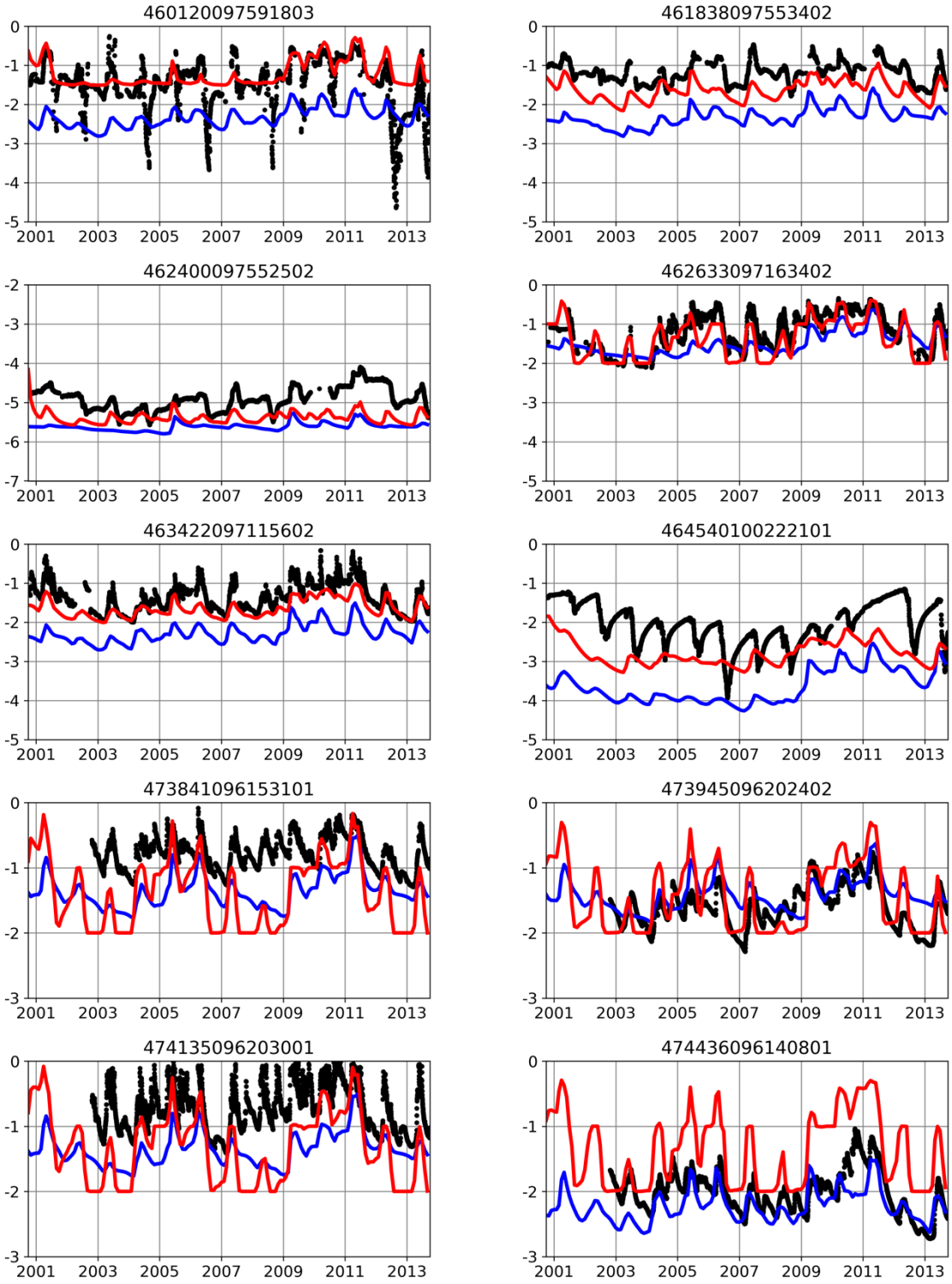
460120097591803
461838097553402
462400097552502
462633097163402
463422097115602
464540100222101
473841096153101
473945096202402
474135096203001
474436096140801

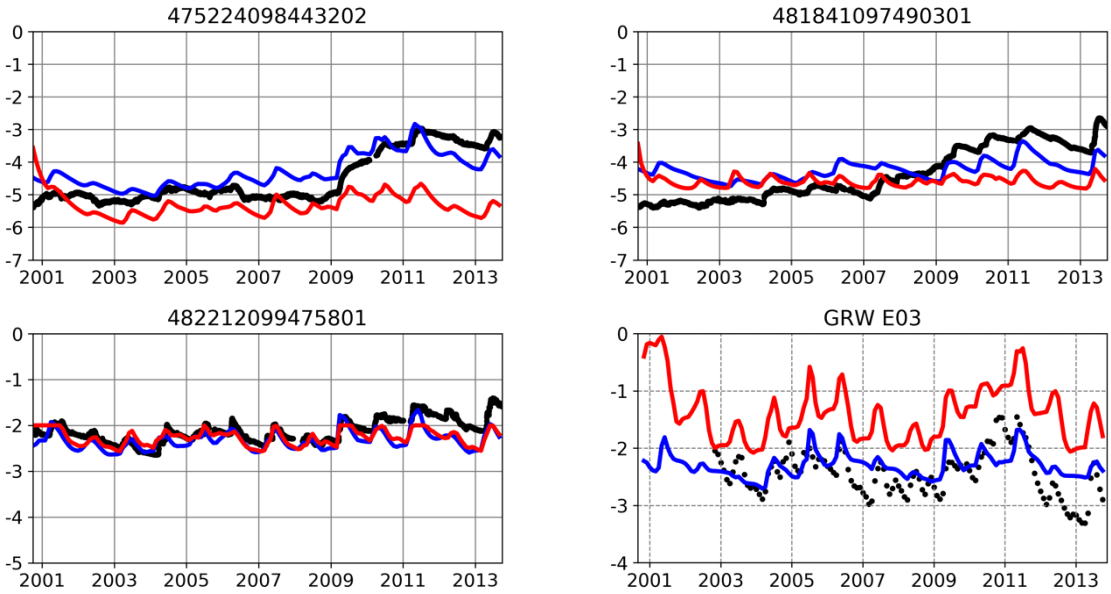

Fig. S4. WTD dynamics from observational wells and CTRL model with default soil (DEF, blue lines) and replacing default soil with sandy soil (REP, red lines) for the 33 sites in the PPR.

Modeling groundwater responses to climate change in the Prairie Pothole Region

Zhe Zhang[1], Yanping Li[1*], Michael Barlage[2], Fei Chen[2], Gonzalo Miguez-Macho[3], Andrew Ireson[1], Zhenhua Li[1]

[1]*Global Institute for Water Security, University of Saskatchewan, Saskatoon, SK, Canada*

[2]*National Center for Atmospheric Research, Boulder, Colorado, USA*

[3]*Nonlinear Physic Group, Faculty of Physics, Universidade de Santiago de Compostela, Galicia, Spain*

Abstract

Shallow groundwater in the Prairie Pothole Region (PPR) is recharged predominantly by snowmelt in the spring and supplies water for evapotranspiration through the summer and fall. This two-way exchange is underrepresented in current land surface models. Furthermore, the impacts of climate change on the groundwater recharge rates are uncertain. In this paper, we use a coupled land and groundwater model to investigate the hydrological cycle of shallow groundwater in the PPR and study its response to climate change at the end of the 21st century. The results show that the model reasonably simulates the water table depth (WTD) and the timing of recharge processes, but predicts deep WTD in mountainous region in Alberta. The most significant change under future climate conditions occurs in the winter, when warmer temperature changes the rain/snow partitioning, delaying the time for snow accumulation/soil freezing while bring forward early melting/thawing. Such changes lead to an earlier start to a longer recharge season, but with lower recharge rates. Different signals are shown in the eastern and western PPR in the future summer, with reduced precipitation and drier soils in the east but little change in the west. The annual recharge increased by 25% and 50% in the eastern and western PPR, respectively. Additionally, we found the mean and seasonal variation of the simulated WTD are sensitive to soil properties and fine-scale soil information is needed to improve groundwater simulation on regional scale.

Keywords: Groundwater, Recharge, Climate Change, Prairie Pothole Region, Hydrological Cycle,

Deleted: may

Deleted: y

Deleted: /

Deleted: -

Deleted: underestimates

Deleted: the seasonal variation of WTD

Deleted: , due to mismatches of the soil types between observations and the model.

Introduction

The Prairie Pothole Region (PPR) in North America is located in a semi-arid and cold region, where evapotranspiration (ET) exceeds precipitation (PR) in summer and near-surface soil is frozen in winter (Gray, 1970; Granger and Gray, 1989; Hayashi et al., 2003; Pomeroy et al., 2007; Ireson et al., 2013; Dumanski et al., 2015). These climatic conditions have introduced unique hydrological characters to the groundwater flow in the PPR (Ireson et al., 2013). During winters, frozen soils reduce permeability and snow accumulates on the surface, prohibiting infiltration (Niu and Yang 2006; Mohammed et al., 2018). At the same time, the water table slowly declines due to a combination of upward transport to freezing front by the capillary effect and discharge to rivers (Ireson et al., 2013). In early springs, snowmelt becomes the dominant component of the hydrological cycle and the melt water runs over frozen soil, with little infiltration contributing to recharge. As the soil thaws, the increased infiltration capacity allows snowmelt recharge to the water table, the previously upward water movement by capillary effect to reverse and move downwards, and the water table to rise to its maximum level. In summers and falls, when high ET exceeds PR, capillary rise may draw water from the groundwater aquifers to supply ET demands, declining water table. These processes characterize the two-way water exchange between sub-surface soils and groundwater aquifers.

Previous studies have suggested that substantial changes to groundwater interactions with above soils are likely to occur under climate change (Tremblay et al., 2011; Green et al., 2011; Ireson et al., 2013, 2015). Existing modeling studies on the impacts of climate change on groundwater are either at global or basin/location-specific scales (Meixner et al., 2016). Global-level groundwater studies focus on potential future recharge trends (Doll and Fiedler, 2008; Doll, 2009), yet coarse

Deleted: ¶

Deleted: [1] Groundwater (GW) is an important source of freshwater for human beings. The domestic needs of about half of the world's population (UNESCO, 2004) and 38% of the global water demand for irrigation are provided by groundwater (Siebert et al., 2010). In the Canadian prairies, more than 30% of the population relied on groundwater in 1996 (Statistics Canada, 1996). In a more recent survey, while 90% of the municipal population is now provided by surface water sources, more than 50% of the population living in rural areas are still relying on groundwater sources in Canada (Environment Canada, 2011). In the U.S., up to 90% of water for drinking and irrigation are provided by groundwater across different parts of the country (National Research Council, 2003).¶

¶

[2] The groundwater flows in cold regions exhibit unique hydrological characteristics due to the hydraulic isolation, induced by seasonally frozen soil (Ireson et al., 2013). As frozen soils reduce permeability and snow accumulates during winter, the timing of groundwater recharge is controlled by the snowmelt and soil thaw period in spring. Previous work by Kelln et al. (2007) found that the timing of the recharge was associated strongly with soil thaw, rather than snowmelt, and occurred one to six weeks later than snowmelt. On the other hand, previous observations in a glacial-till site, where groundwater flow to underlying aquifer and lateral flow are small, have suggested the decline of water table during winter is related to an upward water transport to the freezing front (Remenda et al., 1996). ¶

¶

[3]

Deleted: The groundwater recharge to shallow aquifers in the PPR is crucially influenced by these climatic conditions and seasonal freeze-thaw processes.

Deleted: the

Deleted: snow accumulation and frozen near-surface soil prohibit infiltration.

Deleted: the

Deleted: reaching

Deleted: , the previously upward water movement by capillary effect move downwards, and water table rises to

Deleted: the

Deleted: and desiccates the soil

Deleted: This two-way exchange between unsaturated soils and groundwater aquifers is important for the water table dynamics on regional scale.

Deleted: ¶

[4] Furthermore, groundwater exchange with prairie pothole wetlands are complicated and critical in the PPR. Numerous wetlands known as potholes or sloughs provide important ecosystem services, such as providing wildlife habitats and groundwater recharge (Johnson et al., 2010). Shallow groundwater aquifers may receive water from or lose water to prairie wetlands depending on the hydrological setting. ... [1]

Deleted: [5]

resolution analysis from global climate models (GCMs) provided insufficient specificity to inform decision making. Basin-scale groundwater studies connect the climate with groundwater-flow models to understand the climate impacts on specific systems (Maxwell and Kollet, 2008; Kurylyk and MacQuarrie, 2013; Dumanski et al., 2015). However, a knowledge gap exists in predicting the effect of climate change over large regions (major river basins, states or group of states) (Christensen et al., 2004; Green et al., 2011; Niraula et al., 2017).

Therefore, the objectives of this paper is to investigate the hydrological changes in groundwater in PPR under climate change and understand the drivers for different hydrological processes. Our goals are: 1) to model the water table dynamics in the PPR using a coupled land-groundwater model; 2) to capture changes in the groundwater regime under climate change; and 3) to identify major climatic and land surface processes that contribute to these changes in the PPR.

However, modeling the groundwater flows in PPR using LSMs is challenging because the important two-way water exchange between unsaturated soils and groundwater aquifers was neglected in previous LSMs. Recently, this two-way exchange has been implemented in coupled land surface – groundwater models (LSM-GW). For example, Maxwell and Miller (2005) used a groundwater model (ParFlow) coupled with the Common Land Model (CLM). They found that the coupled and uncoupled model is very similar in simulated sensible heat flux (SH), ET, and shallow soil moisture (SM), but are different greatly in runoff and deep SM. This is perhaps because only downwards flow from soil to groundwater is considered. Later on, Kollet and Maxwell (2008) incorporated the ET effect on redistributing moisture upward from shallow water table depth (WTD) and found the surface energy partition is highly sensitive to a WTD ranging

Deleted: little

Deleted: The lack of climate-groundwater studies at regional scale may be due to two reasons: first, it is challenging to represent the two-way water exchange in coupled land surface and groundwater model at a regional scale; and second, a regional coupled land-hydrology model requires fine-resolution and good quality meteorological forcing, which needs to be further downscaled from GCMs.

Deleted: ¶

Deleted: ¶
[6]

Deleted: e

Deleted: , but is still challenging to apply to cold regions

from 1 – 5 m. More recently, Niu et al. (2011) implemented a simple groundwater model (SIMGM, Niu et al., 2007), into the community Noah LSM with multi-parameterization options (Noah-MP LSM), by adding an unconfined aquifer at the bottom of soil layers.

On the other hand, the soil freeze-thaw processes in cold region winters further complicate this two-way exchange. Previous field studies have found that frozen soil not only influences the timing and amount of downward recharge to aquifers by reducing the soil permeability (Koren et al., 1999; Niu et al., 2006; Kelln et al., 2007), but may also induces upward water transport from aquifers to soil freezing fronts (Spaans and Baker, 1996; Remenda et al., 1996; Hansson et al., 2004). In the modeling community, there is a rich history in the frozen soil parameterizations. Earlier LSMs assumed no significant heat transfer and soil water redistribution for sub-freezing temperature, for example, in simplified SiB and BATS (Xue et al., 1991; Dickinson et al., 1993; Niu and Zeng, 2012). Koren et al. (1999) suggested that the frozen soil is permeable due to marcopores exist in soil structural aggregates, such as cracks, dead root passages, and worm holes. The NoahV3 adopted this scheme as its default option. Niu and Yang (2006) suggested to separate a model grid into frozen and unfrozen patches, and these two patches have a linear effect on the soil hydraulic properties. This treatment was incorporated into CLM 3.0 and Noah-MP in 2007 and 2011, respectively.

Additionally, the spatial heterogeneity of soil moisture and WTD requires high-resolution meteorological input that direct outputs from GCMs are too coarse to provide. Furthermore, in GCMs, great uncertainties of simulated precipitation stem from choice of convection parameterization schemes (Sherwood et al., 2014; Prein et al., 2015). An important approach to

Deleted: In order to reasonably capture the groundwater regime in the PPR under semi-arid and seasonally frozen soil climatic conditions, a coupled LSM-GW with the ability of addressing the two-way exchange between soil and groundwater as well as representing the freeze-thaw process is necessary.

Deleted: ¶

Deleted: [7]

Deleted:

Deleted: In addition to representing the two-way water exchange, …

Deleted:

Deleted: forcing in high spatial resolution,

Deleted: are not available from

Deleted: of coarse resolution

Deleted: in GCMs

Deleted: For example, convective precipitation, an important source of precipitation in the PPR in summer, its frequency, diurnal cycle and propagation are poorly captured by GCM's parameterizations (Rasmussen et al., 2017).

improve precipitation simulation is to conduct dynamical downscale using the convection-permitting model (CPM) (Ban et al., 2014; Prein et al., 2015; Liu et al., 2017). The CPM uses a high spatial resolution (usually under 5-km) to explicitly resolve convection without activating convection parameterization schemes. CPMs can also improve the representation of fine-scale topography and spatial variations of surface fields (Prein et al., 2013). These CPM added-values provide an excellent opportunity to investigate water table dynamics in the PPR.

In this paper, we use a physical process-based LSM (Noah-MP) coupled with a groundwater dynamics model (MMF model). The coupled Noah-MP-MMF model is driven by two sets of meteorological forcing for 13 years under current and future climate scenarios. These two sets of meteorological dataset are from a CPM dynamical downscale project using the Weather Research & Forecast (WRF) model with 4-km grid spacing covering the Contiguous U.S. and Southern Canada (WRF CONUS, Liu et al., 2017). The paper is structured as follow: Section 2 introduces the groundwater observations for WTD evaluation in the PPR, the coupled Noah-MP-MMF model, and the meteorological forcing from the WRF CONUS project. Section 3 evaluates the model simulated WTD timeseries and shows the groundwater budget and hydrological changes due to climate change. Section 4 and 5 offer a broad discussion and conclusion.

Deleted: to

Deleted: e

Deleted: in the atmosphere

Deleted: and not

Deleted: e

Deleted: On the other hand,

Deleted: groundwater

Deleted: evolution

Deleted: ¶

Deleted: [8] Therefore, the purpose of this paper is to investigate the hydrological changes in groundwater in PPR under climate change and understand the drivers for different hydrological processes. Our goal is to 1) simulate the two-way water exchange in the PPR using a coupled land-groundwater model, 2) capture changes in the groundwater regime under climate change, and 3) identify major climatic and land surface processes that contribute to these changes in the PPR. We use a deterministic distributed physical process-based LSM (Noah-MP LSM) coupled with a groundwater dynamics model, called the MMF model (developed by Fan et al. (2007) and Miguez-Macho et al. (2007)). The coupled Noah-MP-MMF model is driven by two sets of meteorological forcing for 13 years under current and future climate scenarios. These two sets of meteorological dataset are from a CPM dynamical downscale project using the Weather Research & Forecast (WRF) model with 4-km grid spacing in the Contiguous U.S. (WRF CONUS, Liu et al., 2017). ¶

¶

[9]

Deleted: al data

Deleted: against observations

Deleted: to the paper

2. Data and Methods

2.1 Observational data

Groundwater observation data were obtained through several agencies: (1) the United States Geological Survey (USGS) National Water Information System in the U.S. (https://waterdata.usgs.gov/nwis/gw), (2) the Alberta Environment (http://aep.alberta.ca/water/programs-and-services/groundwater/groundwater-observation-well-network/default.aspx), (3) the Saskatchewan Water Security Agency (https://www.wsask.ca/Water-Info/Ground-Water/Observation-Wells/).

Initially, groundwater data from 160 wells were acquired, 72 in the U.S., 43 from Alberta, and 45 from Saskatchewan. We used the following criteria to select qualified stations for our study and evaluate our model performance against these observations:

1) the location of the wells are close to the PPR region;
2) a sufficiently long record during the simulation period. We define the observation availability as the available observation period within the 13-year simulation period and select wells with observation availability greater than 80%;
3) unconfined aquifers with shallow groundwater levels (mean WTD > - 5 m);
4) minimal anthropogenic effects (such as pumping or irrigation).

These criteria reduced the observation data to the record of 32 well records, with six in Alberta, 13 in Saskatchewan and 14 from the U.S. **Table 1** summarizes the information for each selected well, and **Fig. 1**(a) shows the location of the wells in our study area. It is noteworthy that most of the groundwater sites have more permeable deposits (sand and gravel) as provincial and state

Deleted: [10]
Deleted: uv?referred_module=gw&search_criteria=search_site_no&search_criteria=site_tp_cd&submitted_form=introduction…
Field Code Changed
Deleted: /
Deleted: , and (4) the Manitoba Water Stewardship Division (https://manitoba.maps.arcgis.com/apps/webappviewer/index.html?id=28fc1a53c9f8435d897501724766a992).
Deleted: 6
Deleted: 40
Deleted: 56
Deleted: 61
Deleted: , and nine from Manitoba.
Deleted: ¶
¶
[11] Despite the data acquired from a large number of wells, not all of the wells were suitable for the study of shallow groundwater and climate change.
Deleted: of groundwater measurement record
Deleted: ;
Deleted: ;
Deleted: unconfined aquifers with shallow groundwater levels (top 7 meters below surface).¶
Formatted: Normal, Left, Indent: Left: 0.63 cm, Line spacing: single, No bullets or numbering
Deleted: ¶
Deleted: 11
Deleted: one
Deleted: six
Deleted: four
Deleted: in Minnesota (
Deleted:).

agencies don't monitor low permeability formation. More information about the selecting criteria are provided in the supplemental materials.

Fig. 1 (a) Topography of the Prairie Pothole Region (PPR) and station location of rain gauges (black dots) and groundwater wells (red diamonds); (b) Topography of the WRF CONUS domain, with the black box indicating the PPR domain.

Table 1. Summary of the locations and aquifer type and soil type of the 33 selected wells.

Deleted: **Table 1** Summary of the locations and aquifer type and soil type of the 11 selected wells.¶

2.2 Groundwater and Frozen Soil Scheme in Noah-MP

In the present study, we used the community Noah-MP LSM (Niu et al. 2011; Yang et al. 2011), coupled with a GW model – the MMF model (Fan et al. 2007; Miguez-Macho et al., 2007). This coupled model has been applied in many regional hydrology studies in offline mode (Miguez-Macho and Fan 2012; Martinez et al., 2016) and coupled with regional climate models (Anyah et al., 2008; Barlage et al., 2015). We present here a brief introduction to the MMF groundwater scheme and the frozen soil scheme in Noah-MP, further details can be found in previous studies (Fan et al., 2007; Miguez-Macho et al., 2007; Niu and Yang, 2006).

Fig. 2 is a diagram of the structure of 4 soil layers (0.1, 0.3, 0.6 and 1.0 m) and the underlying unconfined aquifer in Noah-MP-MMF. The MMF scheme defines explicitly an unconfined aquifer below the 2-m soil and an auxiliary soil layer stretching to the WTD, which varies in space and time [m]. The thickness of this auxiliary layer (z_{aux} [m]) is also variable, depending on the WTD:

$$z_{aux} = \begin{cases} 1, & WTD \geq -3 \\ -2 - WTD, & WTD < -3 \end{cases} \quad (1)$$

The vertical fluxes include gravity drainage and capillary flux, solved from the Richards' equation,

$$q = K_\theta * \left(\frac{\partial \psi}{\partial z} - 1\right), \quad K_\theta = K_{sat} * \left(\frac{\theta}{\theta_{sat}}\right)^{2b+3}, \quad \psi = \psi_{sat} * \left(\frac{\theta_{sat}}{\theta}\right)^{b} \quad (2)$$

where q is water flux between two adjacent layers [m/s], K_θ is the hydraulic conductivity [m/s] at certain soil moisture content θ [m^3/m^3], ψ is the soil capillary potential [m] and b is soil pore size index. The subscript *sat* denote saturated state. Therefore, the recharge flux from/to the layer above WTD, R, can be obtained according to WTD:

Deleted: [12]
Deleted: ,
Deleted: as well as
Deleted: and
Deleted: [13]
Deleted: f Noah-MP
Deleted: MMF
Deleted: The active 2-m soil in Noah-MP LSM consists of 4 layers whose thicknesses (*dz*) are 0.1, 0.3, 0.6 and 1.0 m.
Deleted: [14] Fig. 2 shows the soil layers of NoahMP coupled MMP groundwater scheme.
Deleted: *SMC*
Deleted: *Ψ*
Deleted: *SMC*
Deleted: *SAT*
Deleted: *SMC*
Deleted: *SMCSAT*
Deleted: *Ψ*
Deleted: *Ψ*
Deleted: *SAT*
Deleted: *SMCSAT*
Deleted: *SMC*
Deleted: *SAT*
Deleted: whose values are from the default Noah-MP soil tables…

$$R = \begin{cases} K_k * \left(\frac{\psi_i - \psi_k}{z_{soil(i)} - z_{soil(k)}} - 1\right), & WTD \geq -2 \\ K_{aux} * \left(\frac{\psi_4 - \psi_{aux}}{(-2) - (-3)} - 1\right), & -2 > WTD \geq -3 \\ K_{sat} * \left(\frac{\psi_{aux} - \psi_{sat}}{(-2) - (WTD)} - 1\right), & WTD < -3 \end{cases} \quad (3)$$

In the first case, WTD is in the resolved soil layers and z_{soil} is the depth of soil layer with the subscript k indicating the layer containing WTD while i the layer above. The calculated water table recharge is then passed to the MMF groundwater routine.

The change of groundwater storage in the unconfined aquifer considers three components: recharge flux, river flux, and lateral flows:

$$\Delta S_g = (R - Q_r + \sum Q_{lat}) \quad (4)$$

where S_g [mm] is groundwater storage, Q_r [mm] is the water flux of groundwater-river exchange, and $\sum Q_{lat}$ [mm] are groundwater lateral flows to/from all surrounding grid cells. The groundwater lateral flow ($\sum Q_{lat}$) is the total horizontal flows between each grid cell and its neighbouring grid cells, calculated from Darcy's law with the Dupuit–Forchheimer approximation (Fan and Miguez-Macho 2010), as:

$$Q_{lat} = wT\left(\frac{h - h_n}{l}\right) \quad (5)$$

where w is the width of cell interface [m], T is the transmissivity of groundwater flow [m^2/s], h and h_n are the water table head [m] of local and neighboring cell, and l is the length [m] between cells. T depends on hydraulic conductivity K and WTD:

Deleted: [15]

Deleted: (Fan et al., 2007; Miguez-Macho et al., 2007)

$$T = \begin{cases} \int_{-\infty}^{h} K\,dz & WTD \geq -2 \\ \int_{-\infty}^{(z_{surf}-2)} K\,dz + \sum K_i * dz_i & WTD < -2 \end{cases} \quad (7)$$

For WTD< -2, K is assumed to decay exponentially with depth, $K = K_4 \exp(-z/f)$, K_4 is the hydraulic conductivity in the 4-th soil layer and f is the e-folding length and depends on terrain slope. For WTD ≥ -2, i represents the number of layers between the water table and the 2-m bottom and z_{surf} is the surface elevation.

The river flux (Q_r) is also represented by a Darcy's law–type equation, which is the gradient between the groundwater head, local riverbed depth and parameterized river conductance:

$$Q_r = RC \cdot (h - z_{river}) \quad (8)$$

with z_{river} is the depth of river bed [m] and RC is dimensionless river conductance, which depends on the slope of the terrain and equilibrium water table (*eqzwt,* [m]). Eq. (7) is a simplification which uses z_{river} rather than the water level in the river and, for this study, we only consider one-way discharge from groundwater to rivers. Finally, the change of WTD is calculated as the total fluxes fill or drain the pore space between saturation and the equilibrium soil moisture state (θ_{eq} [m^3/m^3]) in the layer containing WTD:

$$\Delta\text{WTD} = \frac{\Delta S_g}{(\theta_{sat} - \theta_{eq})} \quad (9)$$

If ΔS_g is greater than the pore space in the current layer, the soil moisture content of current layer is saturated and the WTD rises to the layer above, updating the soil moisture content in the layer above as well. Vice versa for negative ΔS_g as water table declines and soil moisture decreases.

Deleted: [16]

Deleted: *SMCSAT*

Deleted: *SMCEQ*

Fig. 2 Structure of the Noah-MP LSM coupled with MMF groundwater scheme, the top 2-m soil of 4 layers whose thicknesses are 0.1, 0.3, 0.6 and 1.0 m. An unconfined aquifer is added below the 2-m boundary, including an auxiliary layer and the saturated aquifer. Positive flux of *R* denotes downward transport. Two water table are shown, one within the 2-m soil and one below, indicating that the model is capable to deal with both shallow and deep water table.

There are two options in Noah-MP LSM for frozen soil permeability; option 1, the default option in Noah-MP, is from Niu and Yang (2006) and option 2 is inherited the Koren et al. (1999) scheme from NoahV3. Option 1 assumes that a model grid cell consists of permeable and impermeable patches and these patches integrate a linear effect on soil hydraulic properties. Thus, the total soil moisture in the grid cell is used to compute hydraulic properties as:

$$\theta = \theta_{ice} + \theta_{liq}$$

$$K = (1 - F_{frz})K_u = (1 - F_{frz})K_{sat}(\frac{\theta}{\theta_{sat}})^{2b+3}$$

$$\psi = \psi_u = \psi_{sat}(\frac{\theta}{\theta_{sat}})^{-b}$$

the subscript *frz* and u denote the frozen and unfrozen patches in the grid point. The water flux within in a model grid cell is:

$$q = (1 - F_{frz})q_u + F_{frz}q_{frz}$$

And the impermeable frozen soil fraction is parameterized as:

$$F_{frz} = e^{-\alpha(1-\theta_{ice}/\theta_{sat})} - e^{-\alpha}$$

α = 3.0 is an adjustable parameter.

However, the option 2 uses only the liquid water volume to calculate hydraulic properties and assumes a non-linear effect of frozen soil on permeability. Generally, option 1 assumes that soil ice has a smaller effect on infiltration and simulates more permeable frozen soil than option 2 (Niu et al., 2011). For this reason, the option 1 allows the soil water to move and redistribute more easily within the frozen soil and we decide to use option 1 in our study.

Deleted: is consist

Deleted: depth

Deleted: as well as

Formatted: Font: Times New Roman, 10 pt, Font color: Auto

Formatted: Space After: 0 pt, Line spacing: Double

Formatted: Font: 10 pt

Formatted: Font: 10 pt

Formatted: Default Paragraph Font, Font: 10 pt

Formatted: Font: 10 pt

Formatted: Font: 10 pt

Formatted: Default Paragraph Font, Font: 10 pt

Formatted: Font: 10 pt

Formatted: Default Paragraph Font, Font: 10 pt

Formatted: Default Paragraph Font, Font: 10 pt, Italic

Formatted: Default Paragraph Font, Font: 10 pt

Formatted: Default Paragraph Font, Font: 10 pt

Formatted: Justified, Line spacing: Double

Formatted: Default Paragraph Font, Font: 10 pt

Formatted: Font: Times New Roman, 10 pt, Font color: Auto

Formatted: Font: 10 pt

Formatted: Default Paragraph Font, Font: 10 pt

Formatted: Font: 10 pt

2.3 Forcing Data

The output from the WRF CONUS dataset (Liu et al. 2017) are used as meteorological forcing to drive the Noah-MP-MMF model. The WRF CONUS project consists of two simulations. The first simulation is referred as the current climate scenario, or control run (CTRL), from Oct 2000 to Sep 2013, and forced with the 6-hourly 0.7° ERA-Interim reanalysis data. The second simulation is a perturbation to reflect the future climate scenario, closely following the pseudo global warming (PGW) approach in previous works (Rasmussen et al., 2014). The PGW simulation is forced with 6-hourly ERA-Interim reanalysis data plus a delta climate change signal derived from an ensemble of CMIP5 models under the RCP8.5 emission scenario and reflects the climate change signal between the end of 21st and 20th century.

Fig. 3 shows the annual precipitation in the PPR from 4-km WRF CONUS from the current climate and 32-km North America Regional Reanalysis (NARR, another reanalysis dataset commonly used for land surface model forcing). Both datasets show similar annual precipitation pattern and bias patterns compared to observations: underestimating of precipitation in the east and overestimating in the west. However, the WRF CONUS shows significant improvement of percentage bias in precipitation ((Model-Observation)/Observation) over the western PPR. For the consistency of the same source of data for current and future climate, the WRF-CONUS is the best available dataset for the coupled land-groundwater study in the PPR.

Fig. 3 Evaluation of the annual precipitation from WRF CONUS (top) and NARR (bottom) against rain gauge observation.

Deleted: [17] We use
Deleted: t
Deleted: atmospheric forcing
Deleted: simulation
Deleted:
Deleted: simulation
Deleted: part
Deleted: :
Deleted: one
Deleted: is
Deleted: downscaled
Deleted: from
Deleted: data
Deleted: ;
Deleted: t
Deleted: other is
Deleted: the
Deleted: as the future climate scenario
Deleted: ,
Deleted: which
Deleted: adds
Deleted: delta climate change signal
Formatted: Superscript
Formatted: Superscript
Formatted: Font: Times New Roman
Deleted: . ¶ ¶ [18]
Deleted: To also address
Deleted: using
Deleted: we believe
Deleted: 4-km
Deleted:
Deleted: is
Deleted: to drive the
Deleted: model.

For the future climate study, the precipitation and temperature of the PGW climate forcing are shown in **Fig. 4** and **Fig. 5**. The WRF CONUS projects more precipitation in the PPR, except in the southeast of the domain in summer, where it shows a precipitation reduction of about 50 to 100 mm. On the other hand, the WRF CONUS projects strongest warming occurring in the northeast PPR in winter (**Fig. 5**), about 6–8 °C. Another significant warming signal occurs in summer in the southeast of domain, corresponding to the reduction of future precipitation, as seen in **Fig. 4**.

Deleted: [19]

Deleted: – warming of

Fig. 4 Seasonal accumulated precipitation from current climate scenario(CTRL), future climate scenario (PGW) and projected change (PGW-CTRL) in the forcing data.

Fig. 5 Seasonal averaged temperature from CTRL, PGW, and the projected change (PGW-CTRL)

Deleted: Same as **Fig. 4** but for 2-m air temperature.

2.4 Model Setup

The two Noah-MP-MMF simulations representing the current climate and future climate are denoted as CTRL and PGW, respectively. The initial groundwater levels are from a global 1-km equilibrium groundwater map (Fan et al., 2013) and the equilibrium soil moisture for each soil layer is calculated at the first model timestep with climatology recharge, spinning up for 500 years. Since the model domain is at a different resolution than the input data, the appropriate initial WTD at 4-km may be different than the average at 1-km. To properly initialize the simulation, we spin up the model using the forcing of current climate (CTRL) for the years from 2000 to 2001 repeatedly (in total 10 loops).

Due to different data sources, the default soil types along the boundary between the U.S. and Canada are discontinuous. Thus, we use the global 1-km fine soil data (Shangguan et al., 2014, http://globalchange.bnu.edu.cn/research/soilw) in our study region. The soil properties for the aquifer use the same properties as the lowest soil layer from the Noah-MP 2-m soil layers.

Deleted: [20]

Deleted: The CTRL simulation starts from Oct 2000 and end in Sep 2013, consist of 13 water years. The PGW simulation corresponds to the same period of time, but under climate change scenario at the end of 21st century.¶ ¶ [21]

Deleted: model's initial groundwater

Deleted: is

Deleted: 4

Deleted: ¶

Deleted: [22]

Deleted: The coupled Noah-MP-MMF groundwater model is configured using the default 2-m depth with 4 layers.

3. Results

3.1 Comparison with groundwater observations

According to the locations of 33 groundwater wells in **Table 1**, the simulated WTD from the closest model grid points are extracted. **Fig. 6** shows the modeled WTD bias from the CTRL run. We also select the monthly WTD timeseries from 8 sites, the observation are in black dots and CTRL in blue lines. See supplemental materials for the timeseries of 33 sites. The model produces reasonable values of mean WTD, the mean bias are smaller than 1 m in most of sites, except in Alberta, where the model predicts deep bias in mountainous region. The model also successfully captures the annual cycle of WTD, which rises in spring and early summer, because of snowmelt and rainfall recharge, and declines in summer and fall, because of high ET, and in winter because of frozen near-surface soil. In all observations, the timing of water table rising and dropping is well simulated, as the timing and amount of infiltration and recharge in spring is controlled by the freeze-thaw processes in seasonally frozen soil.

Fig. 6. WTD (m) bias from CTRL simulation and timeseries from 8 groundwater wells in PPR. See Table 2 CTRL column for the model statistics and supplemental materials for complete timeseries from 33 wells.

On the other hand, the model simulated WTD seasonal variation is smaller than observations. The small seasonal variation could be due to the misrepresentation between the lithology from the observational surveys and the soil types in the model grids. As mentioned in Section 2.2, the groundwater aquifer uses the same soil types as the bottom layer of the resolved 2-m soil layers. While sand and gravel are the dominant lithology in most of the sites, they are mostly clay and loam in the model (Table 1). For sandy soil reported in most of the sites, small capacity and fast responses to infiltration lead to large water table fluctuations, whereas, in the model, clay and loam soil allows low permeability and large capacity, and smoothens responses to recharge and capillary

Deleted: [23]
Deleted: 11
Deleted: t
Deleted: ed WTD
Deleted: (
Deleted: plus)
Deleted: simulated
Deleted: monthly WTD (
Deleted:) in the study domain
Deleted: These processes are reasonably captured by the frozen soil scheme in Noah-MP LSM (Niu et al., 2006; Niu et al., 2011).…
Deleted: **Fig. 6** WTD (m) from 11 groundwater wells and the model simulation results in the PPR. ¶
Deleted: [24]
Deleted: match
Deleted: soil properties of the unconfined
Deleted: are the
Deleted: except for silt in Crater Lake,
Deleted: and drainage

effects. Furthermore, the 4-layer soils are vertically homogeneous in soil type and the groundwater model uses the lowest level soil type as the aquifer lithology. For many part of the PPR, where groundwater level are perched at the top 5-m due to a layer called glacial till. This geohydrological characteristics cannot be reflected in this model and contribute to the deep WTD bias simulated in Alberta. This shortcoming of the model was also reported in a study taken place in the Amazon rainforest (Miguez-Macho et al., 2012).

Deleted: ¶
[25] Despite mismatches between the model and sites in topography and soil properties at high spatial resolution, this out-of-the-box simulation of the Noah-MP MMF groundwater scheme shows reasonable results, as shown in **Fig. 6**. Therefore, we consider the simulated WTD satisfactory in the mean, seasonal, and interannual dynamics, and are reliable for further study of climate change impacts on groundwater in the PPR.¶

3.2 Climate change signal in Groundwater fluxes

The MMF groundwater model simulates three components in the groundwater water budget, the recharge flux (R), lateral flow (Q_{lat}), and discharge flux to rivers (Q_r). Because the topography is usually flat in the PPR, the magnitude of groundwater lateral transport is very small (Q_{lat} less than 5 mm per year). On the other hand, the shallow water table in the PPR region is higher than the local river bed, thus, the Q_r term is always discharging from groundwater aquifers to rivers. As a result, the recharge term is the major contributor to the groundwater storage in the PPR, and its variation (usually between -100 to 100 mm) dominates the timing and amplitude of the water table dynamics. The seasonal accumulated total groundwater fluxes in the PPR ($R+Q_{lat}-Q_r$) are shown in **Fig. 7**. The positive (negative) flux in blue (red) means the groundwater aquifer is gaining (losing) water, causing the water table to rises (decline).

Fig. 7 Seasonal accumulated total groundwater fluxes ($R+$) for current climate (CTRL, top), future climate (PGW, middle) and projected change (PGW-CTRL, bottom) in forcing data. Black dashed lines in PGW-CTRL separate the PPR into eastern and western halves.

Under current climate conditions, the total groundwater flux show strong seasonal fluctuations, consistent with the WTD timeseries shown in **Fig. 6**. On average, in fall (SON) and winter (DJF), there is a 20-mm negative recharge, driven by the capillary effects and drawing water from aquifer to dry soil above. Spring (MAM) is usually the season with a strong positive recharge because snowmelt provides a significant amount of water, and soils thawing allow infiltration. The large amount of snowmelt water contributes to more than 100 mm of positive recharge in the eastern domain. It is until summer (JJA), when strong ET depletes soil moisture and results in about 50 mm of negative recharge.

Deleted: [26]

Deleted: negative and

Deleted: +

Deleted: (blue)

Deleted: ; and the negative flux (red) indicates the aquifer is losing water and the water table is declining.

Deleted: **Fig. 7** Same as **Fig. 3** but for total groundwater fluxes (R + -). ¶

Deleted: [27]

643 Under future climate conditions, the increased PR in fall and winter leads to wetter upper soil
644 layers, resulting in a net positive recharge flux (PGW – CTRL in SON and DJF). However, the
645 PGW summer is impacted by increased ET under a warmer and drier climate, due to higher
646 temperature and less PR. As a result, the groundwater uptake by the capillary effect is more critical
647 in the future summer. Furthermore, there is a strong east-to-west difference in the total
648 groundwater flux change from PGW to CTRL. In the eastern PPR, the change in total groundwater
649 flux exhibits obvious seasonality while the model projects persistent positive groundwater fluxes
650 in the western PPR.
651

Deleted: [28]

3.3 Water budget analysis

Fig. 8 and **Fig. 9** show the water budget analysis for the eastern and western PPR (divided by the dotted line in 103° W in Fig. 7), respectively. Four components are presented in the figures, i.e. (1) PR and ET; (2) surface and underground runoff (*SFCRUN* and *UDGRUN*); and surface snowpack; (3) the change of soil moisture storage and (4) groundwater fluxes and the change of storage. In current and future climate, these budget terms are plotted in annual accumulation ((a) and (b) for CTRL and PGW), whereas their difference are plotted in each month individually ((c) for PGW-CTRL).

Under current climate conditions, during snowmelt infiltration and rainfall event, water infiltrates into the top soil layer, travels through the soil column and exits the bottom of the 2-m boundary, hence, the water table rises. During the summer dry season, ET is higher than PR and the soil layers lose water through ET, therefore, the capillary effect takes water from the underlying aquifer and the water table declines. In winter, the near-surface soil in the PPR is seasonally frozen, thus, a redistribution of subsurface water to the freezing front results in negative recharge, and the water table declines.

In the eastern PPR, the effective precipitation (PR-ET) is found to increase from fall to spring, but decrease in summer in PGW (**Fig. 8**(1c)). Warmer falls and winters in PGW, together with increased PR, not only delay snow accumulation and bring forward snowmelt, but also change the precipitation partition – more as rain and less as snow. This warming causes up to 20 mm of snowpack loss (**Fig.8**(2c)). The underground runoff starts much earlier in PGW (December) (**Fig.8**(2b)) than in CTRL (February) (**Fig.8**(2a)). On the other hand, the warming in PGW also

Deleted: [29]

Deleted: [30]

Deleted: D

Deleted: s when ET demand is low

Deleted:

Deleted: [31]

Deleted: results in later time for

Deleted: earlier for

Deleted: ing

Deleted: s

changes the partitioning of soil ice and soil water in subsurface soil layers (**Fig**. 8(3c)). For late spring in PGW, the springtime recharge in the future is significantly reduced due to early melting and less snowpack remaining (**Fig. 8**(4c)). In the PGW summer, reduced PR (50 mm less) and higher temperatures (8 °C warmer) lead to reduction in total soil moisture, and a stronger negative recharge from the aquifer. Therefore, the increase of recharge from fall to early spring compensates the recharge reduction due to stronger ET in summer in the eastern PPR, and changes little in the annual mean groundwater storage (1.763 mm per year).

Fig. 8 Water budget analysis in the eastern PPR in (a) CTRL, (b) PGW and (c) PGW – CTRL. Water budget terms include: (1) *PR & ET*, (2) surface snow, surface runoff and underground runoff (*SNOW*, *SFCRUN*, and *UDGRUN*), (3) change of soil moisture storage (soil water, soil ice and total soil moisture, ΔSMC) and (4) groundwater fluxes and the change of groundwater storage (R, Q_{lat}, Q_r, ΔS_g). The annual mean soil moisture change (PGW-CTRL) is shown with black dashed line in (3). The Residual term is defined as $Res = (R+Q_{lat}-Q_r)-\Delta S_g$ in (4). Note that in (a) and (b) the accumulated fluxes and change in storage are shown in lines, whereas in (c) the difference in (PGW-CTRL) is shown for each individual month in bars.

These changes in water budget components in the western PPR (**Fig. 9**) are similar to those in the eastern PPR (**Fig. 8**), except in summer. The reduction in summer PR in the western the PPR (less than 5 mm reduction) is not as obvious as that in the eastern PPR (50 mm reduction) (**Fig. 4**). Thus, annual mean total soil moisture in future is about the same as in current climate (Fig. 9(3c)) and results in little negative recharge in PGW summer (**Fig. 9**(4c)). Therefore, the increase in annual recharge is more significant (10 mm per year), an increase of about 50% of the annual recharge in the current climate (20 mm per year) (**Fig. 9**(4c)).

Deleted: [32]

Fig. 9 Same as **Fig. 8**, but for the western PPR.

In both the eastern and western PPR, the water budget components for the groundwater aquifer are plotted in **Fig. 8**(4) and **Fig. 9** (4), with the changes of each flux (PGW-CTRL) printed at the bottom. The groundwater lateral flow is a small term in areal average and has little impact on the groundwater storage. Nearly half of the increased recharge in both the eastern and western PPR is discharged to river flux (Q_r = 2.26 mm out of R = 4.15 mm in the eastern PPR and Q_r = 5.20 mm out of R = 10.72 mm in western PPR). Therefore, the groundwater storage change in the eastern PPR (1.76 mm per year) is not as great as that in the western PPR (5.39 mm per year).

These two regions of the PPR show differences in hydrological response to future climate because of the spatial variation of the summer PR. As shown in both **Fig. 4** (PGW-CTRL), **Fig. 8**(1) and **Fig. 9**(1), the reduction of future PR in summer in the eastern PPR is significant (50 mm). The spatial difference of precipitation changes in the PPR further results in the recharge increase doubling in the western PPR compared to the eastern PPR.

Deleted: [33]

Deleted: [34]

4. Discussion

4.1 Improving WTD Simulation

In Section 3.1, we show that model is capable of simulating the mean WTD in most sites, yet predicts deep groundwater in Alberta and underestimates its seasonal variation. These results may be due to misrepresentations between model default soil type and the soil properties in the observational wells. To test this theory, an additional simulation, REP, is conducted by replacing the default soil types in the locations of these 33 groundwater wells with sand-type soil, which is the dominant soil types reported from observational surveys. The timeseries of the REP and default CTRL are shown in Fig. 10 (also see supplemental materials for the complete 33 sites) and a summary of the mean and standard deviation of the two simulations are provided in Table 2.

Fig. 10 Same as Fig. 6, the timeseries of simulated WTD from both default model (blue) and replacing soil type simulation, REP (red). REP is the additional simulation by replacing the default soil type in the model with sandy soil type.

The REP simulation with sandy soil show two sensitive signals: (1) REP WTD are shallower than the default simulation; (2) and exhibit stronger seasonal variation. These two signals can be explained by the WTD equation in the MMF scheme:

$$\Delta WTD = \frac{\Delta(R + Q_{lat} - Q_r)}{(\theta_{sat} - \theta_{eq})} \quad (10)$$

Eq. (10) represents that the change of WTD in a period of time is calculated by the total groundwater fluxes, $\Delta(R + Q_{lat} - Q_r)$, divided by the available soil moisture capacity of current layer ($\theta_{sat} - \theta_{eq}$). In REP simulation, the parameters θ_{sat} for the dominant soil type in observational sites (sand/gravel) is smaller than those in default model grids (clay loam, sandy loam, loam, loamy sand, etc.). Therefore, changing the θ_{sat} is essentially reducing the storage in

Deleted: Simulated
Deleted: sensitivity to soil property parameters
Deleted: [35]
Deleted: matche
Deleted: 11
Deleted: sites
Deleted: .
Deleted:
Deleted: (MOD)
Deleted: Fig. 10 Same as Fig. 6, the time series of simulated WTD from both default model (MOD) and replacing soil type simulation (REP). ¶
Deleted: [36]
Deleted: type
Deleted: from observational surveys
Deleted: (red lines in Fig. 10)
Deleted: REP WTD timeseries
Deleted: shows
Deleted: +
Deleted: *SMCSAT*
Deleted: *SMCEQ*
Deleted: where *SMCMAX* is the maximum soil moisture capacity in the current layer, a parameter determined by the soil type. …
Deleted: +
Deleted: *SMCMAX* − *SMCEQ*
Deleted:
Deleted: *SMCSAT*
Deleted: *SMCSAT*
Deleted: alter

783 the aquifer and soil in this model grid. Given the same amount of groundwater flux, in the REP
784 simulation, the mean WTD is higher and the seasonal variation is stronger than the default CTRL
785 run.

786

787 In the REP simulation, we replaced soil type only at a limited number of sites because the
788 geological survey data in high resolution and large area extent is not yet available for the whole
789 PPR. At point scale, the WTD responses to climate change over these limited number of sites show
790 diverse results and uncertainties (see supplemental materials). For the rest of the domain, the
791 default soil type from global 1-km soil map is used. The REP modifications of soil types at point-
792 scale have small contribution to the water balance analysis (Fig. 8 & 9) at regional-scale. Our
793 results and conclusions for groundwater response to PGW doesn't change. We are currently
794 undertaking a soil property survey project in the PPR region to obtain soil properties at high spatial
795 resolution, both horizontal and vertical. This may provide better opportunity to improve WTD
796 simulation as well as assess climate-groundwater interaction in future studies.

797

798 4.2 Climate change Impacts on Groundwater Hydrological Regime

799 Climate change induced warming in high-latitudes winter and increased precipitation, including a
800 higher liquid fraction, in PGW winter results in later snow accumulation, higher winter recharge
801 and earlier melting in spring. Such changes in snowpack loss have been hypothesized in
802 mountainous as well as high-latitude regions (Taylor et al 2013; Ireson et al., 2015; Meixner et al.,
803 2016; Musselman et al., 2017).

804

Deleted: than the default run and the seasonal variation is stronger, hence, increasing the WTD seasonal variation.¶

Deleted: [37] We show the REP simulation in order to prove our theory in Section 3.1, that the simulated WTD is sensitive to parameters associated soil properties, and thus could be improved by obtaining more realistic soil maps.

Deleted: But i

Deleted: with observations

Deleted: these 11

Deleted: locations

Deleted: Future development in fine-scale soil properties will hopefully improve the WTD simulation.

Deleted: [38]

Deleted: On an annual basis, the coupled model projects substantial increases in recharge, 25% in eastern and 50% in western PPR.

In addition to the amount of recharge, the shift of recharge season is also noteworthy. Under current climate conditions in spring, soil thawing (in March) is generally later than snowmelt (in February) by a month in the PPR. Thus, the snowmelt water in pre-thaw spring would either re-freeze after infiltrating into partially frozen soil or become surface runoff. Under the PGW climate, the warmer winter and spring allows snowmelt and soil thaw to occur earlier in the middle of winter (in January and February, respectively). As a result, the recharge season starts earlier in December, and last longer until June, results in longer recharge season but with lower recharge rate.

Future projected increasing evapotranspiration demand in summer desiccates soil moisture, resulting in more water uptake from aquifers to subsidize dry soil in the future summer. This groundwater transport to soil moisture is similar to the "buffer effect" documented in an offline study in the Amazon rainforest (Pokhrel et al., 2014). In , shallow water tables exist in the critical zone, where WTD ranges from 1 to 5 meters below surface and could exert strong influence on land energy and moisture fluxes feedback to the atmosphere (Kollet and Maxwell, 2008; Fan , 2015). Previous coupled atmosphere-land-groundwater studies at 30-km resolution showed that groundwater could support soil moisture during summer dry period, but has little impacts on precipitation in Central U.S. (Barlage et al., 2015). It would be an interesting topic to study the integrated impacts of shallow groundwater to regional climate in the convection permitting resolution (resolution < 5-km).

4.3 Fine-scale interaction between groundwater and Prairie pothole wetlands

Furthermore, groundwater exchange with prairie pothole wetlands are complicated and critical in the PPR. Numerous wetlands known as potholes or sloughs provide important ecosystem services,

Deleted: [39]

Deleted: [40]

Deleted: stronger

Deleted: upper

Deleted: layers

Deleted: upper

Deleted: upper

Deleted: layers

Deleted: both Amazon rainforest and the PPR

Deleted: from

Deleted: (Kollet and Maxwell, 2008; Fan , 2015)

such as providing wildlife habitats and groundwater recharge (Johnson et al., 2010). Shallow groundwater aquifers may receive water from or lose water to prairie wetlands depending on the hydrological setting. Depression-focused recharge generated by runoff from upland to depression contributes to sufficient amount of water input to shallow groundwater (5-40 mm/year) (Hayashi et al., 2016).

On the other hand, groundwater lateral flow exchange center of a wetland pond to its moist margin is also an important components in the wetland water balance (van der Kamp and Hayashi, 2009; Brannen, et al., 2015; Hayashi et al., 2016). However, this groundwater-wetland exchange typically occurs on local scale (from 10 to 100 m) and thus, is challenging to in current land surface models or climate models (resolution from 1 km to 100 km). In this paper, we focus on the groundwater dynamics on regional scale, therefore, still unable to capture these small wetland features in our model. We admit this challenge and are currently developing a sub-grid scheme to represent open water wetlands as a fraction in a grid cell and calculate its feedback to regional environments. Future studies on this topic will provide valuable insights on these key ecosystems and their interaction under climate change.

Formatted: Font: Times, Font color: Black

Conclusion

In this study, a coupled land-groundwater model is applied to simulate the interaction between the groundwater aquifer and soil moisture in the PPR. The climate forcing is from a dynamical downscaling project (WRF CONUS), which uses the convection-permitting model (CPM) configuration in high resolution. The goal of this study is to investigate the groundwater responses to climate change, and to identify the major processes that contribute to these responses in the PPR. To our knowledge, this is the first study applying CPM forcing in a hydrology study in this region. We have three main findings:

(1) the coupled land-groundwater model shows reliable simulation of mean WTD, however underestimates the seasonal variation of the water table against well observations. This could be attributed to several reasons, including misrepresentation of topography and soil types, as well as vertical homogenous soil layers used in the model. We further conducted an additional simulation (REP) by replacing the model default soil types with sand-type soil, and the simulated WTDs were improved in both mean and seasonal variation. However, inadequacy of soil properties in deeper layer and higher spatial resolution is still a limitation.

(2) Recharge markedly increases due to projected increased PR, particularly from fall to spring under future climate conditions. Strong east-west spatial variation exists in the annual recharge increases, 25% in the eastern and 50% in the western PPR. This is due to the significant projected PR reduction in PGW summer in the eastern PPR but little change in the western PPR. This PR reduction leads to stronger ET demand, which draws more groundwater uptake due to the capillary effect, results in negative recharge in the summer. Therefore, the increased recharge from fall to

Deleted: [41] The fluctuation of the shallow WTD and recharge are closely related to the semi-arid climatic condition and seasonally frozen soil in the Prairie Pothole Region (PPR). The freeze-thaw processes and effective precipitation are critical factors to the magnitude and timing for snowmelt infiltration in spring, groundwater uptake in summer and moisture redistribution in winter. The two-way water exchange between soil layers and groundwater aquifer is essential to the groundwater regime in the PPR. ¶
¶
[42] Previous works on modeling climate change impacts on groundwater, at both global or local basin scale, have been limited by precipitation uncertainties stemming from choice of convection parameterization in GCMs. (Green et al., 2011; Kurylyk et al., 2013; Taylor et al., 2013; Smerdon 2017). Additionally, these models typically neglected the two-way exchange of water flux between soil and aquifers, which has been a historical simplification in the coupled land-groundwater model. ¶
¶
[43]

Deleted: our

Deleted: high spatial resolution

Deleted: To our knowledge, this is the first study applying convection-permitting regional climate model (RCM) forcing in a hydrology study.

Deleted: [44]

Deleted: This is mostly due to the mismatches of soil types between groundwater sites and corresponding model grid points. This mismatch comes from inadequate information of aquifer parameters, which are the same as those for the lowest soil layer.

Deleted: demonstrated in

Deleted: default

Deleted: observational “true” value

Deleted: that

Deleted: the simulated WTD is sensitive to soil type parameters, and …

Deleted: (< -2 m)

Deleted: [45]

Deleted: In general,

Deleted: r

Deleted: results in

Deleted: As a results

spring is consumed by ET in summer, and results in little change in groundwater in the eastern PPR, while gaining water in the western PPR.

(3) The timing of infiltration and recharge are critically impacted by the changes in freeze-thaw processes. Increased precipitation, combined with higher winter temperatures, results in later snow accumulation/soil freezing, partitioned more as rain than snow, and earlier snowmelt/soil thaw. This leads to substantial loss of snowpack, shorter frozen soil season, and higher permeability in soil allowing infiltration. Late accumulation/freezing and early melting/thawing leads to an early start of a longer recharge season from December to June, but with a lower recharge rate.

Our study has some limitations where future studies are encouraged:

(1) Despite the large number of groundwater wells in PPR, only a few are suitable for long-term evaluation, due to data quality, anthropogenic pumping, and length of data record. As remote sensing techniques advance, observing terrestrial water storage anomalies derived from the GRACE satellite may provide substantial information on WTD, although the GRACE information needs to be downscaled to a finer scale before comparisons can be made with regional hydrology models at km-scale (Pokhrel et al., 2013).

(2) This study is an offline study of climate change impacts on groundwater. It is important to investigate how shallow groundwater in the earth's critical zone could interact with surface water and energy exchange to the atmosphere and affect regional climate. This investigation would be important to the central North America region (one of the land atmosphere coupling "hot spots", Koster et al., 2004).

Deleted: storage

Deleted: higher storage

Deleted: [46]

Deleted: temperature-induced

Deleted: in the future winter

Deleted: Additionally,

Deleted: l

Deleted: [47]

Deleted: needed

Deleted: [48]

Acknowledgments

The authors Zhe Zhang, Yanping Li, Zhenhua Li gratefully acknowledge the support from the Changing Cold Regions Network (CCRN) funded by the Natural Science and Engineering Research Council of Canada (NSERC), as well as the Global Water Future project and Global Institute of Water Security at University of Saskatchewan. Yanping Li acknowledge the support from NSERC Discovery Grant. Fei Chen, Michael Barlage appreciate the support from the Water System Program at the National Center for Atmospheric Research (NCAR), USDA NIFA Grants 2015-67003-23508 and 2015-67003-23460, NSF INFEW/T2 Grant #1739705, and NOAA CFDA Grant #NA18OAR4590381. NCAR is sponsored by the National Science Foundation. Any opinions, findings, conclusions or recommendations expressed in this publication are those of the authors and do not necessarily reflect the views of the National Science Foundation.

Deleted: ¶
Page Break
¶

Reference

Anyah, R. O., Weaver, C. P., Miguez-macho, G., Fan, Y. and Robock, A.: Incorporating water table dynamics in climate modeling : 3 . Simulated groundwater influence on coupled land-atmosphere variability, , 113, 1–15, doi:10.1029/2007JD009087, 2008.

Ban, N., Schmidli, J. and Schär, C.: Evaluation of the new convective-resolving regional climate modeling approach in decade-long simulations, J. Geophys. Res. Atmos., 119, 7889–7907, doi:10.1002/2014JD021478.Received, 2014.

Barlage, M., Tewari, M., Chen, F., Miguez-Macho, G., Yang, Z. L. and Niu, G. Y.: The effect of groundwater interaction in North American regional climate simulations with WRF/Noah-MP, Clim. Change, 129(3–4), 485–498, doi:10.1007/s10584-014-1308-8, 2015.

Brannen, R., Spence, C. and Ireson, A.: Influence of shallow groundwater-surface water interactions on the hydrological connectivity and water budget of a wetland complex, Hydrol. Process., 29(18), 3862–3877, doi:10.1002/hyp.10563, 2015.

Christensen NS, Wood AW, Voisin N, et al (2004) The Effects of Climate Change on the Hydrology and Water Resources of the Colorado River Basin. Clim Change 62:337–363. doi: 10.1023/B:CLIM.0000013684.13621.1f

Dickinson RE, Henderson-Sellers A, Kennedy PJ (1993) Biosphere-Atmosphere Transfer Scheme (BATS) Version le as Coupled to the NCAR Community Climate Model. NCAR Technical Note, NCAR/TN-387+STR.

Döll, P. and Fiedler, K.: Global-scale modeling of groundwater recharge, Hydrol. Earth Syst. Sci., 12(3), 863–885, doi:10.5194/hess-12-863-2008, 2008.

Döll, P.: Vulnerability to the impact of climate change on renewable groundwater resources: A global-scale assessment, Environ. Res. Lett., 4(3), doi:10.1088/1748-9326/4/3/035006, 2009.

Dumanski, S., Pomeroy, J. W. and Westbrook, C. J.: Hydrological regime changes in a Canadian Prairie basin, Hydrol. Process., 29(18), 3893–3904, doi:10.1002/hyp.10567, 2015.

Environment Canada: Municipal Water Use, 2009 Statistics, 2011 Munic. Water Use Rep., 24, doi:En11-2/2009E-PDF Information, 2011.

Fan Y, Miguez-Macho G, Weaver CP, et al (2007) Incorporating water table dynamics in climate modeling: 1. Water table observations and equilibrium water table simulations. J Geophys Res Atmos 112:1–17. doi: 10.1029/2006JD008111

Fan, Y., Li, H. and Miguez-Macho, G.: Global patterns of groundwater table depth, Science (80-.)., 339(6122), 940–943, doi:10.1126/science.1229881, 2013.

Fan, Y.: Groundwater in the Earth's critical zones: Relevance to large-scale patterns and processes, Water Resour. Res., 3052–3069, doi:10.1002/2015WR017037.Received, 2015.

Granger RJ, Gray DM: Evaporation from natural non-saturated surface. J. Hydrol., 111, 21–29, 1989.

Gray DM: Handbook on the Principles of Hydrology: With Special Emphasis Directed to Canadian Conditions in the Discussion, Applications, and Presentation of Data. Water Information Center: Huntingdon, New York, 1970. ISBN:0-912394-07-2

Green, T. R., Taniguchi, M., Kooi, H., Gurdak, J. J., Allen, D. M., Hiscock, K. M., Treidel, H. and Aureli, A.: Beneath the surface of global change: Impacts of climate change on groundwater, J. Hydrol., 405(3–4), 532–560, doi:10.1016/j.jhydrol.2011.05.002, 2011.

Hayashi, M., Van Der Kamp, G. and Schmidt, R.: Focused infiltration of snowmelt water in partially frozen soil under small depressions, J. Hydrol., 270(3–4), 214–229, doi:10.1016/S0022-1694(02)00287-1, 2003.

Hayashi, M., van der Kamp, G. and Rosenberry, D. O.: Hydrology of Prairie Wetlands: Understanding the Integrated Surface-Water and Groundwater Processes, Wetlands, 36, 237–254, doi:10.1007/s13157-016-0797-9, 2016.

Ireson, A. M., van der Kamp, G., Ferguson, G., Nachshon, U. and Wheater, H. S.: Hydrogeological processes in seasonally frozen northern latitudes: understanding, gaps and challenges, Hydrogeol. J., 21(1), 53–66, doi:10.1007/s10040-012-0916-5, 2013.

Ireson, A. M., Barr, A. G., Johnstone, J. F., Mamet, S. D., van der Kamp, G., Whitfield, C. J., Michel, N. L., North, R. L., Westbrook, C. J., DeBeer, C., Chun, K. P., Nazemi, A. and Sagin, J.: The changing water cycle: the Boreal Plains ecozone of Western Canada, Wiley Interdiscip. Rev. Water, 2(5), 505–521, doi:10.1002/wat2.1098, 2015.

Johnson, W. C., Werner, B., Guntenspergen, G. R., Voldseth, R. A., Millett, B., Naugle, D. E., Tulbure, M., Carroll, R. W. H., Tracy, J. and Olawsky, C.: Prairie Wetland Complexes as Landscape Functional Units in a Changing Climate, Bioscience, 60(2), 128–140, doi:10.1525/bio.2010.60.2.7, 2010.

Kelln C, Barbour L, Qualizza C (2007) Preferential Flow in a Reclamation Cover : Hydrological and Geochemical Response. 1277–1289

Koren, V., Schaake, J., Mitchell, K., Duan, Q.-Y., Chen, F., & Baker, J. M. (1999). A parameterization of snowpack and frozen ground intended for NCEP weather and climate models. Journal of Geophysical Research: Atmospheres, 104(D16), 19569–19585. https://doi.org/10.1029/1999JD900232

Koster, R. D., Dirmeyer, P. A., Guo, Z., Bonan, G., Chan, E., Cox, P., Gordon, C. T., Kanae, S., Kowalczyk, E., Lawrence, D., Liu, P., Lu, C.-H., Malyshev, S., McAvaney, B., Mitchell, K., Mocko, D., Oki, T., Oleson, K., Pitman, A., Sud, Y. C., Taylor, C. M., Verseghy, D., Vasic, R., Xue, Y. and Yamada, T.: Regions of Strong Coupling Between Soil Moisture and Precipitation, Science (80-.)., 305(5687), 1138 LP-1140 [online] Available from: http://science.sciencemag.org/content/305/5687/1138.abstract, 2004.

Kollet SJ, Maxwell RM (2008) Capturing the influence of groundwater dynamics on land surface processes using an integrated, distributed watershed model. Water Resour Res 44:1–18. doi: 10.1029/2007WR006004

Kurylyk, B. L. and MacQuarrie, K. T. B.: The uncertainty associated with estimating future groundwater recharge: A summary of recent research and an example from a small unconfined aquifer in a northern humid-continental climate, J. Hydrol., 492, 244–253, doi:10.1016/j.jhydrol.2013.03.043, 2013.

Liu, C., Ikeda, K., Rasmussen, R., Barlage, M., Newman, A. J., Prein, A. F., Chen, F., Chen, L., Clark, M., Dai, A., Dudhia, J., Eidhammer, T., Gochis, D., Gutmann, E., Kurkute, S., Li, Y., Thompson, G. and Yates, D.: Continental-scale convection-permitting modeling of the current and future climate of North America, Clim. Dyn., 49(1–2), 71–95, doi:10.1007/s00382-016-3327-9, 2017.

Martinez, J. A., Dominguez, F. and Miguez-Macho, G.: Effects of a Groundwater Scheme on the Simulation of Soil Moisture and Evapotranspiration over Southern South America, J. Hydrometeorol., 17(11), 2941–2957, doi:10.1175/JHM-D-16-0051.1, 2016.

Maxwell RM, Miller NL (2005) Development of a Coupled Land Surface and Groundwater Model. 233–247

Maxwell, R. M. and Kollet, S. J.: Interdependence of groundwater dynamics and land-energy feedbacks under climate change, Nat. Geosci., 1(10), 665–669, doi:10.1038/ngeo315, 2008.

Meixner, T., Manning, A. H., Stonestrom, D. A., Allen, D. M., Ajami, H., Blasch, K. W., Brookfield, A. E., Castro, C. L., Clark, J. F., Gochis, D. J., Flint, A. L., Neff, K. L., Niraula, R., Rodell, M., Scanlon, B. R., Singha, K. and Walvoord, M. A.: Implications of projected climate change for groundwater recharge in the western United States, J. Hydrol., 534, 124–138, doi:10.1016/j.jhydrol.2015.12.027, 2016.

Miguez-Macho, G., Fan, Y., Weaver, C. P., Walko, R. and Robock, A.: Incorporating water table dynamics in climate modeling: 2. Formulation, validation, and soil moisture simulation, J.

Miguez-Macho, G. and Fan, Y.: The role of groundwater in the Amazon water cycle: 1. Influence on seasonal streamflow, flooding and wetlands, J. Geophys. Res. Atmos., 117(15), 1–30, doi:10.1029/2012JD017539, 2012.

Moeck, C., Brunner, P. and Hunkeler, D.: The influence of model structure on groundwater recharge rates in climate-change impact studies, Hydrogeol. J., 24(5), 1171–1184, doi:10.1007/s10040-016-1367-1, 2016.

Mohammed, A. A., Kurylyk, B. L., Cey, E. E. and Hayashi, M.: Snowmelt Infiltration and Macropore Flow in Frozen Soils: Overview, Knowledge Gaps, and a Conceptual Framework, Vadose Zo. J., 17(1), doi:10.2136/vzj2018.04.0084, 2018.

Musselman, K. N., Clark, M. P., Liu, C., Ikeda, K. and Rasmussen, R.: Slower snowmelt in a warmer world, Nat. Clim. Chang., 7(February), 214–220, doi:10.1038/NCLIMATE3225, 2017.

National Research Council: Groundwater fluxes across inter- faces. The National Academy Press, 85 pp, 2003

Niraula R, Meixner T, Dominguez F, et al (2017) How Might Recharge Change Under Projected Climate Change in the Western U.S.? Geophys Res Lett 44:10,407-10,418. doi: 10.1002/2017GL075421

Niu, G.-Y., & Yang, Z.-L. (2006). Effects of Frozen Soil on Snowmelt Runoff and Soil Water Storage at a Continental Scale. Journal of Hydrometeorology, 7(5), 937–952. https://doi.org/10.1175/JHM538.1

Niu G, Yang Z, Dickinson RE, Gulden LE (2007) Development of a simple groundwater model for use in climate models and evaluation with Gravity Recovery and Climate Experiment data. 112:1–14. doi: 10.1029/2006JD007522

Niu, G. Y., Yang, Z. L., Mitchell, K. E., Chen, F., Ek, M. B., Barlage, M., Kumar, A., Manning, K., Niyogi, D., Rosero, E., Tewari, M. and Xia, Y.: The community Noah land surface model with multiparameterization options (Noah-MP): 1. Model description and evaluation with local-scale measurements, J. Geophys. Res. Atmos., 116(12), 1–19, doi:10.1029/2010JD015139, 2011.

Niu G-Y, Zeng X (2012) Earth System Model, Modeling the Land Component of. In: Climate Change Modeling Methodology. Springer New York, New York, NY, pp 139–168

Pokhrel, Y. N., Fan, Y., Miguez-Macho, G., Yeh, P. J. F. and Han, S. C.: The role of groundwater in the Amazon water cycle: 3. Influence on terrestrial water storage computations and comparison with GRACE, J. Geophys. Res. Atmos., 118(8), 3233–3244, doi:10.1002/jgrd.50335, 2013.

Pokhrel, Y. N., Fan, Y. and Miguez-Macho, G.: Potential hydrologic changes in the Amazon by the end of the 21st century and the groundwater buffer, Environ. Res. Lett., 9(8), doi:10.1088/1748-9326/9/8/084004, 2014.

Formatted: Font: (Default) Calibri

Formatted: Font: (Default) Times New Roman, 12 pt, Font color: Auto

Formatted: Left, Indent: Left: 0 cm, Hanging: 1 cm

Formatted: Font: Not Italic

Formatted: Font: Not Italic

Pomeroy, J. W.: The cold regions hydrological model: a platform for basing process representation and model structure on physical evidence, Hydrol. Process., 21, 2650–2667, doi:10.1002/hyp, 2007.

Prein, A. F., Gobiet, A., Suklitsch, M., Truhetz, H., Awan, N. K., Keuler, K. and Georgievski, G.: Added value of convection permitting seasonal simulations, , 2655–2677, doi:10.1007/s00382-013-1744-6, 2013.

Prein, A. F., Langhans, W., Fosser, G., Ferrone, A., Ban, N., Goergen, K., Keller, M., Tölle, M., Gutjahr, O., Feser, F., Brisson, E., Kollet, S., Schmidli, J., Van Lipzig, N. P. M. and Leung, R.: A review on regional convection-permitting climate modeling: Demonstrations, prospects, and challenges, Rev. Geophys., 53(2), 323–361, doi:10.1002/2014RG000475, 2015.

Rasmussen, K. L., Prein, A. F., Rasmussen, R. M., Ikeda, K. and Liu, C.: Changes in the convective population and thermodynamic environments in convection-permitting regional climate simulations over the United States, Clim. Dyn., (0123456789), 1–26, doi:10.1007/s00382-017-4000-7, 2017.

Remenda VH, van der Kamp G, Cherry JA (1996) Use of vertical profiles of • 180 to constrain estimates of hydraulic conductivity in a thick, unfractured aquitard. 32:2979–2987

Shangguan W, Dai Y, Duan Q, et al (2014) Journal of Advances in Modeling Earth Systems. J Adv Model Earth Syst 6:249–263. doi: 10.1002/2013MS000293.Received

Sherwood, S. C., Bony, S. and Dufresne, J.: Spread in model climate sensitivity traced to atmospheric convective mixing, , doi:10.1038/nature12829, 2014.

Siebert, S., Burke, J., Faures, J. M., Frenken, K., Hoogeveen, J., Döll, P. and Portmann, F. T.: Groundwater use for irrigation - A global inventory, Hydrol. Earth Syst. Sci., 14(10), 1863–1880, doi:10.5194/hess-14-1863-2010, 2010.

Smerdon, B. D.: A synopsis of climate change effects on groundwater recharge, J. Hydrol., 555, 125–128, doi:10.1016/j.jhydrol.2017.09.047, 2017.

Statistics Canada: Quarterly Estimates of the Population of Canada, the Provinces and the Territories, 11-3, Catalogue 91-001, Ottawa, 1996

Taylor, R. G.: Ground water and climate change, , 3(November 2012), doi:10.1038/NCLIMATE1744, 2013.

Tremblay, L., Larocque, M., Anctil, F. and Rivard, C.: Teleconnections and interannual variability in Canadian groundwater levels, J. Hydrol., 410(3–4), 178–188, doi:10.1016/j.jhydrol.2011.09.013, 2011.

UNESCO: Groundwater Resources of the Wrold and Their Use, edited by I. Zektser and L. Everett, Paris., 2004.

Van Der Kamp G, Hayashi M (2009) Groundwater-wetland ecosystem interaction in the semiarid glaciated plains of North America. Hydrogeol J 17:203–214. doi: 10.1007/s10040-008-0367-1

Xue Y, Sellers PJ, Kinter JL, Shukla J (1991) A Simplified Biosphere Model for Global Climate Studies. J Clim 4:345–364. doi: 10.1175/1520-0442(1991)004<0345:ASBMFG>2.0.CO;2

Yang, Z. L., Niu, G. Y., Mitchell, K. E., Chen, F., Ek, M. B., Barlage, M., Longuevergne, L., Manning, K., Niyogi, D., Tewari, M. and Xia, Y.: The community Noah land surface model with multiparameterization options (Noah-MP): 2. Evaluation over global river basins, J. Geophys. Res. Atmos., 116(12), 1–16, doi:10.1029/2010JD015140, 2011.

Table and Figure

Table 1. Summary of the locations and aquifer type and soil type of the 33 selected wells.

Site Name/ Site No.	Lat	Lon	Elev	Aquifer type	Aquifer Lithology	Model Elevation	Model Soil type
Devon 0162	53.41	-113.76	700.0	Unconfined	Sand	697.366	Sandy loam
Hardisty 0143	52.67	-111.31	622.0	Unconfined	Gravel	633.079	Loam
Kirkpatrick Lake 0229	51.95	-111.44	744.5	Semi-confined	Sandstone	778.311	Sandy loam
Metiskow 0267	52.42	-110.60	677.5	Unconfined	Sand	679.516	Loamy sand
Wagner 0172	53.56	-113.82	670.0	Surficial	Sand	670.845	Silt loam
Narrow Lake 252	54.60	-113.63	640.0	Unconfined	Sand	701.0	Clay loam
Baildon 060	50.25	-105.50	590.184	Surficial	-	580.890	Sandy loam
Beauval	55.11	-107.74	434.3	Intertill	Sand	446.5	Sandy loam
Blucher	52.03	-106.20	521.061	Intertill	Sand/Gravel	523.217	Loam
Crater Lake	50.95	-102.46	524.158	Intertill	Sand/Gravel/Clay	522.767	Loam
Duck Lake	52.92	-106.23	502.920	Surficial	Sand	501.729	Loamy sand
Forget	49.70	-102.85	606.552	Surficial	Sand	605.915	Sandy loam
Garden Head	49.74	-108.52	899.160	Bedrock	Sand/Till	894.357	Clay loam
Nokomis	51.51	-105.06	516.267	Bedrock	Sand	511.767	Clay loam
Shaunavon	49.69	-108.50	896.040	Bedrock	Sand/Till	900.433	Clay loam
Simpson 13	51.45	-105.18	496.620	Surficial	Sand	493.313	Sandy loam
Simpson 14	51.457	-105.19	496.600	Surficial	Sand	493.313	Sandy loam
Yorkton 517	51.17	-102.50	513.643	Surficial	Sand/Gravel	511.181	Loam
Agrium 43	52.03	-107.01	500.229	Intertill	Sand	510.771	Loam
460120097591803	46.02	-97.98	401.177	Alluvial	Sand/Gravel	400.381	Sandy loam
461838097553402	46.31	-97.92	401.168	-	Sand/Gravel	404.719	Clay loam
462400097552502	46.39	-97.92	409.73	-	Sand/Gravel	407.405	Sandy loam
462633097163402	46.44	-97.27	325.52	Alluvial	Sand/Gravel	323.728	Sandy loam
463422097115602	46.57	-97.19	320.40	Alluvial	Sand/Gravel	314.167	Sandy loam
464540100222101	46.76	-100.37	524.91	-	Sand/Gravel	522.600	Clay loam
473841096153101	47.64	-96.25	351.77	Surficial	Sand/Gravel	344.180	Loamy sand
473945096202402	47.66	-96.34	327.78	Surficial	Sand/Gravel	328.129	Sandy loam
474135096203001	47.69	-96.34	325.97	Surficial	Sand/Gravel	327.764	Sandy loam
474436096140801	47.74	-96.23	341.90	Surficial	Sand/Gravel	336.210	Sandy loam
475224098443202	47.87	-98.74	451.33	-	Sand/Gravel	450.463	Sandy loam
481841097490301	48.31	-97.81	355.61	-	Sand/Gravel	359.568	Clay loam
482212099475801	48.37	-99.79	488.65	-	Sand/Gravel	488.022	Sandy loam
CRN Well WLN03	45.98	-95.20	410.7	Surficial	Sand/Gravel	411.4	Sandy loam

Deleted: 11
Formatted Table
Formatted: Centered
Formatted: Centered
Formatted: Centered
Formatted: Centered
Formatted: Centered
Formatted: Centered
Formatted: Centered
Formatted: Centered
Formatted: Centered
Formatted: Centered
Formatted: Centered
Formatted: Centered
Formatted: Centered
Formatted: Centered
Formatted: Centered
Formatted: Centered
Formatted: Centered
Formatted: Centered
Formatted: Centered
Formatted: Centered
Formatted: Centered
Formatted: Centered
Formatted: Centered
Formatted: Centered
Formatted: Centered
Formatted: Centered
Formatted: Centered
Formatted: Centered
Formatted: Centered
Formatted: Centered
Formatted: Centered
Deleted: WELL NAME ... [3]
Deleted: WELL NAME ... [2]
Formatted Table
Formatted Table

Table 2. Summary of mean and standard deviation (std) of WTD from 33 groundwater wells, from observation records (OBS), default model (CTRL) and replacing with sand soil simulation (REP). Bold texts indicate improvement in the REP than the CTRL run.

Site Name/Number	OBS_mean	CTRL_mean	REP_mean	OBS_std	CTRL_std	REP std
Devon 0162	-2.46	-2.69	**-2.38**	0.43	0.45	0.09
Hardisty 0143	-2.44	-8.91	**-6.88**	0.41	0.64	**0.36**
Kirkpatrick Lake 0229	-4.22	-4.03	-3.45	0.43	0.98	**0.22**
Metiskow 0267	-2.54	-5.39	**-4.43**	0.34	0.78	**0.55**
Narrow Lake 252	-2.31	-4.81	**-3.75**	0.28	0.60	0.51
Wagner 0172	-2.14	-8.06	**-2.70**	0.48	0.37	0.21
Baildon 060	-2.80	-3.29	**-3.20**	0.47	0.58	0.30
Beauval	-3.78	-4.85	**-4.20**	0.44	0.56	0.32
Blucher	-2.20	-4.24	**-2.16**	0.3	0.92	**0.26**
Crater Lake	-4.33	-3.97	-3.64	1.1	0.4	0.28
Duck Lake	-3.65	-3.69	-3.17	0.54	0.41	**0.62**
Forget	-2.28	-2.37	**-2.23**	0.33	0.17	0.19
Garden Head	-3.67	-4.85	**-3.77**	0.88	0.70	0.30
Nokomis	-1.04	-2.70	**-2.17**	0.23	0.55	**0.17**
Shaunavon	-1.62	-4.41	**-2.58**	0.42	0.69	0.20
Simpson 13	-4.82	-4.83	-3.02	0.31	0.91	**0.17**
Simpson 14	-2.03	-2.61	**-1.82**	0.34	0.18	**0.27**
Yorkton 517	-2.87	-3.97	**-1.98**	0.8	0.46	0.32
Agrium 43	-2.66	-3.75	**-3.38**	0.32	1.05	**0.36**
460120097591803	-1.44	-2.33	**-1.63**	0.56	0.24	**0.50**
461838097553402	-1.17	-2.32	**-1.68**	0.27	0.24	0.43
462400097552502	-4.9	-5.61	**-5.37**	0.29	0.09	**0.17**
462633097163402	-1.18	-1.49	**-1.02**	0.46	0.29	**0.54**
463422097115602	-1.36	-2.28	**-1.66**	0.34	0.23	0.49
464540100222101	-2.02	-3.64	**-2.78**	0.52	0.43	0.32
473841096153101	-0.77	-1.48	**-1.37**	0.24	0.18	0.51
473945096202402	-1.59	-1.58	-1.56	0.32	0.24	0.51
474135096203001	-0.72	-1.48	**-1.30**	0.33	0.25	0.54
474436096140801	-2.44	-2.29	-1.96	0.39	0.21	**0.40**
475224098443202	-4.52	-4.28	-5.31	0.75	0.52	0.34
481841097490301	-4.39	-4.24	-4.58	0.79	0.28	0.17
482212099475801	-2.13	-2.32	**-2.26**	0.24	0.20	0.17
CRN WLN 03	-2.04	-2.18	-1.88	0.24	0.18	0.43

Deleted: in the parenthesis
Deleted: 11
Deleted: MOD
Deleted: "true"
Deleted: properties
Deleted: EP
Deleted: show
Deleted: mean and seasonal variation of WTD
Deleted: STATION ... [4]
Formatted Table

(a) (b)

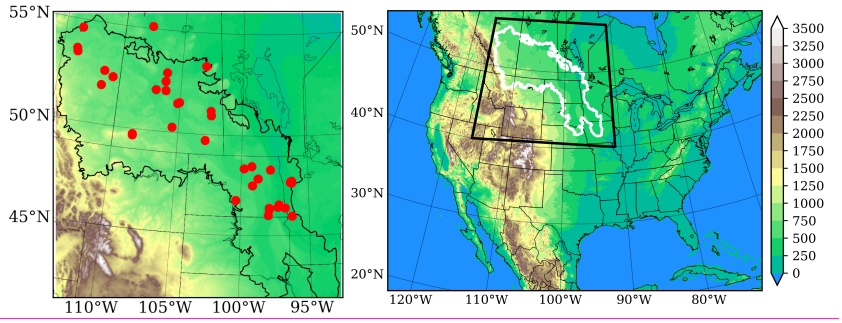

(b)

(c)

Fig. 1 (a) Topography of the Prairie Pothole Region (PPR; black outline) and groundwater wells (red dots); (b) Topography of the WRF CONUS domain, the black box indicates the PPR domain.

Deleted:

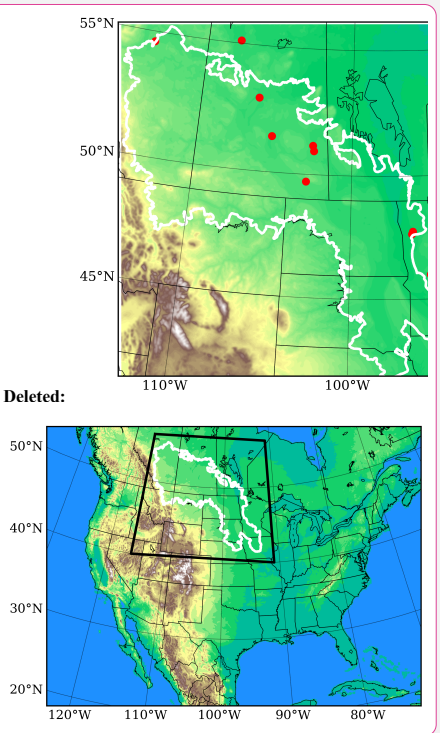

Formatted: List Paragraph, Right: 0 cm, Numbered + Level: 1 + Numbering Style: a, b, c, … + Start at: 1 + Alignment: Left + Aligned at: 0.11 cm + Indent at: 0.74 cm

Deleted: white outline

Deleted: and station location of rain gauges (gray dots)

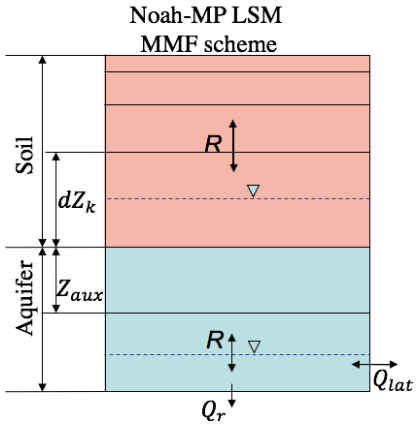

Fig. 2 Structure of the Noah-MP LSM coupled with MMF groundwater scheme, the top 2-m soil of 4 layers whose thicknesses are 0.1, 0.3, 0.6 and 1.0 m. An unconfined aquifer is added below the 2-m boundary, including an auxiliary layer and the saturated aquifer. Positive flux of *R* denotes downward transport. Two water table are shown, one within the 2-m soil and one below, indicating that the model is capable to deal with both shallow and deep water table.

Deleted: Fig. 2 Structure of the Noah-MP LSM coupled with MMF groundwater scheme, the top 2-m soil is consist of 4 layers whose depth are 0.1, 0.3, 0.6 and 1.0 m. An unconfined aquifer is added below the 2-m boundary, including an auxiliary layer and the saturated aquifer. Positive flux of *R* denotes downward transport. Two water table are shown, one within the 2-m soil and one below, indicating that the model is capable to deal with shallow as well as deep water table. ¶

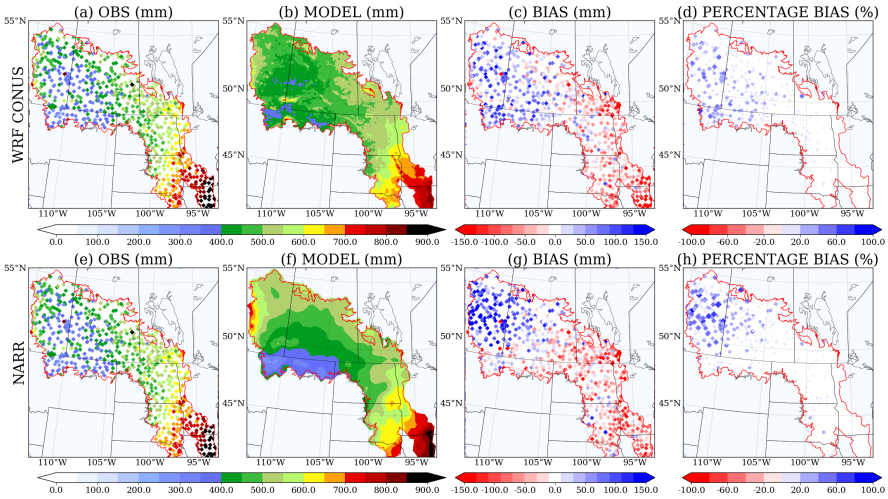

Fig. 3 Evaluation of the annual precipitation from two model products (b, f), WRF CONUS and NARR against rain gauge observation (a, e), their bias (c, g) and percentage bias (d, h).

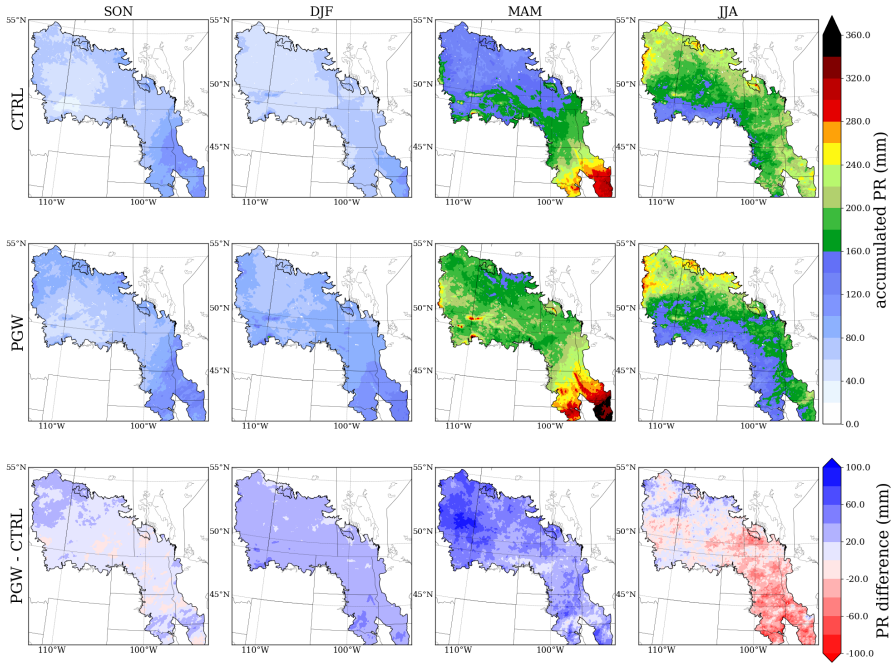

Fig. 4 Seasonal Accumulated precipitation from current climate (CTRL, top), future climate (PGW, middle) and projected change (PGW-CTRL, bottom) in forcing data.

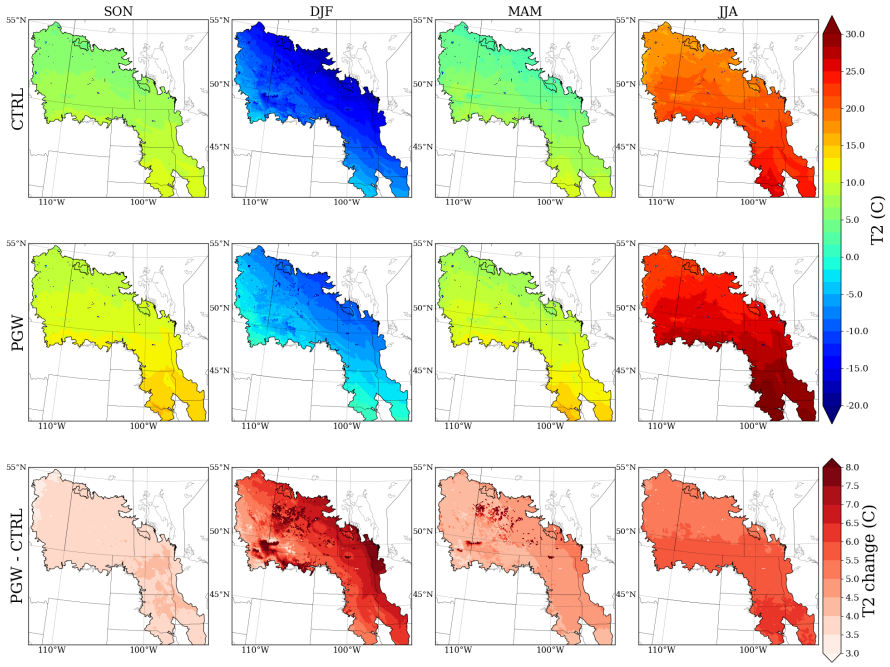

Fig. 5 Seasonal temperatures from current climate (CTRL, top), future climate (PGW, middle) and projected change (PGW-CTRL, bottom) in forcing data.

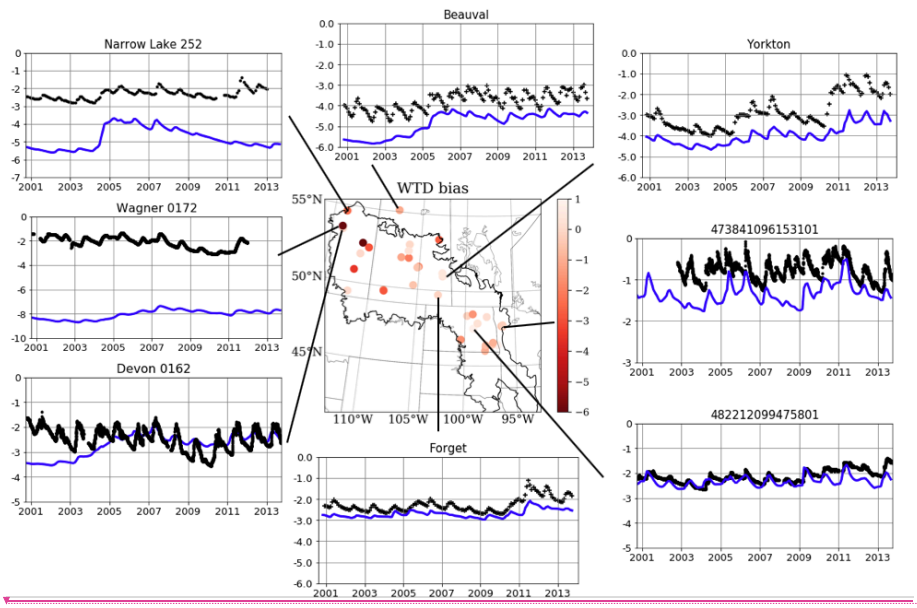

Fig. 6. WTD (m) bias from CTRL simulation and timeseries from 8 groundwater wells in PPR. See Table 2 CTRL column for the model statistics and supplemental materials for complete timeseries from 33 wells.

Deleted:

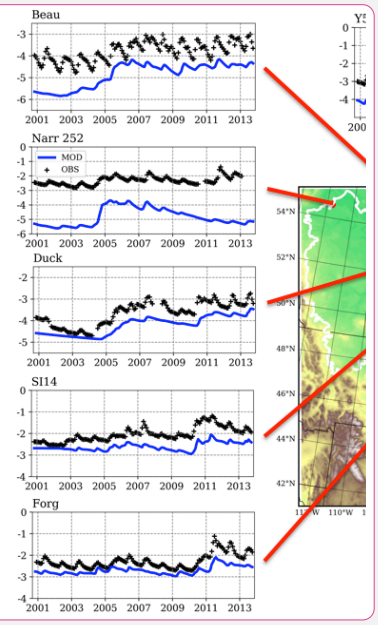

Formatted: Indent: Left: 0 cm, First line: 0 cm

Deleted: from 11

Deleted: and the model simulation results

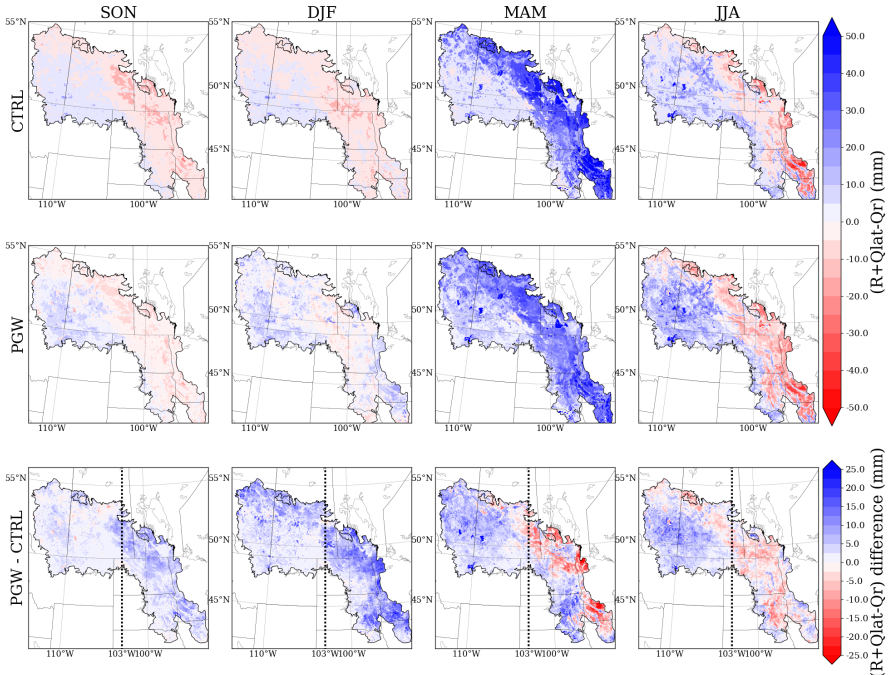

Fig. 7 Seasonal accumulated total groundwater fluxes ($R+Q_{lat}-Q_r$) for current climate (CTRL, top), future climate (PGW, middle) and projected change (PGW-CTRL, bottom) in forcing data. Black dashed lines in PGW-CTRL separate the PPR into eastern and western halves.

Deleted: +

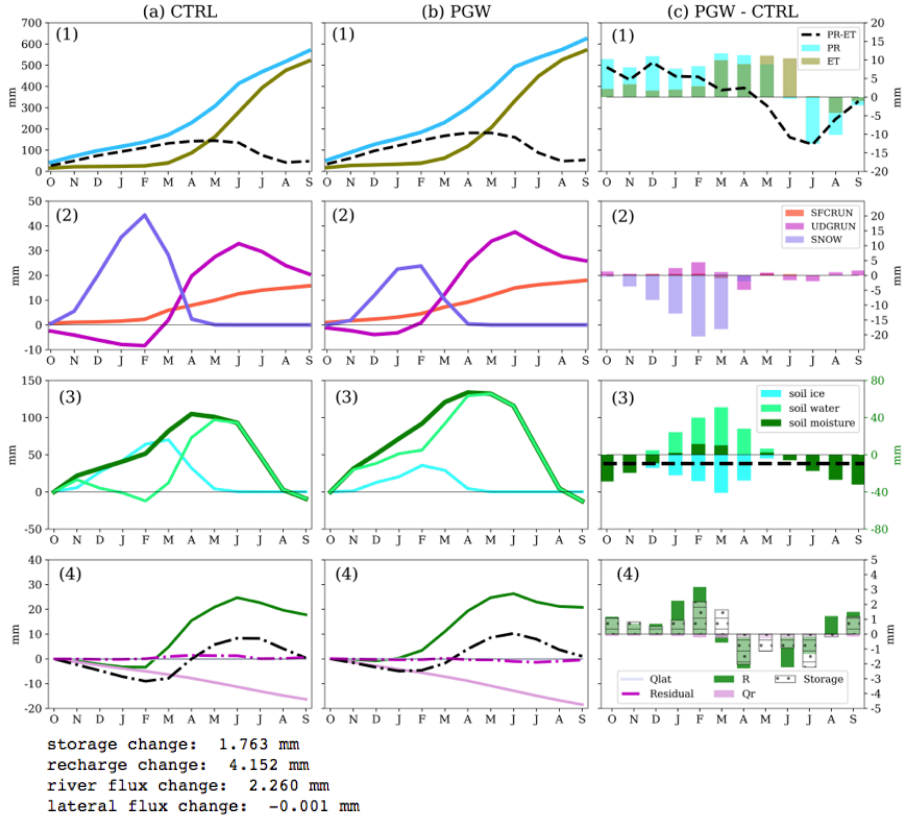

Fig. 8 Water budget analysis in the eastern PPR in (a) CTRL, (b) PGW and (c) PGW – CTRL. Water budget terms include: (1) *PR & ET*, (2) surface snow, surface runoff and underground runoff (*SNOW*, *SFCRUN*, and *UDGRUN*), (3) change of soil moisture storage (soil water, soil ice and total soil moisture, ΔSMC) and (4) groundwater fluxes and the change of groundwater storage (R, Q_{lat}, Q_r, ΔS_g). The annual mean soil moisture change (PGW-CTRL) is shown with black dashed line in (3). The Residual term is defined as $Res = (R+Q_{lat}-Q_r)-\Delta S_g$ in (4). Note that in (a) and (b) the accumulated fluxes and change in storage are shown in lines, whereas in (c) the difference in (PGW-CTRL) is shown for each individual month in bars.

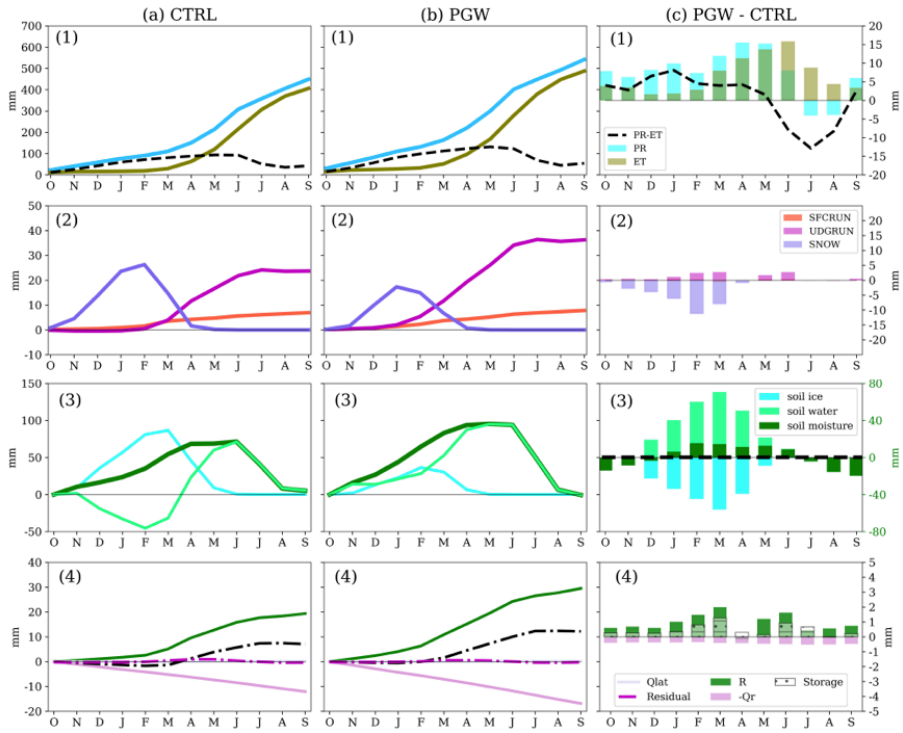

Fig. 9 Same as Fig. 8, but for the **western PPR.**

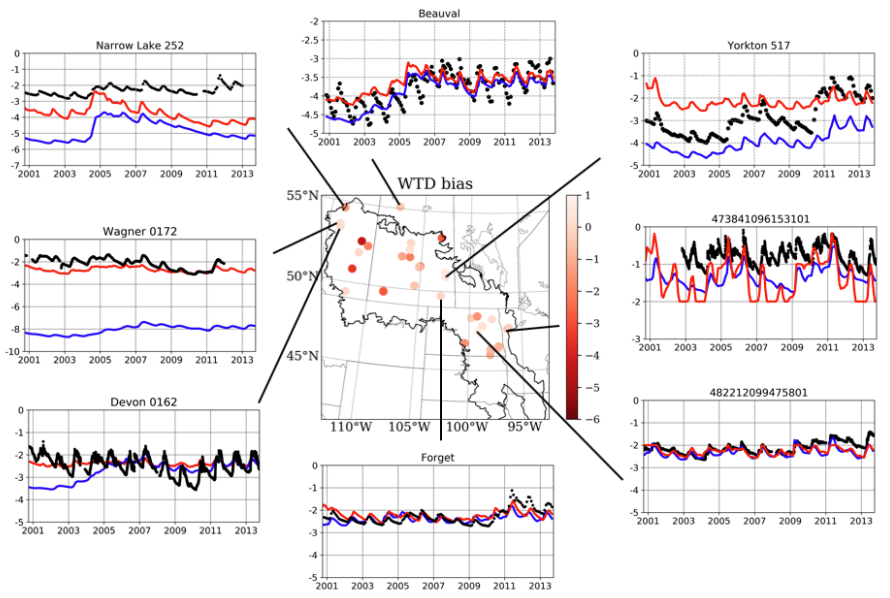

Fig. 10 Same as Fig. 6, the timeseries of simulated WTD from both default model (blue) and replacing soil type simulation, REP (red), REP is the additional simulation by replacing the default soil type in the model with sandy soil type.

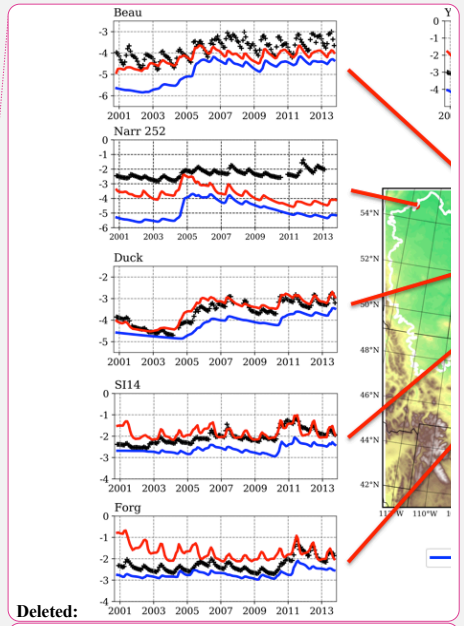

Deleted:

Deleted: ¶

Deleted: MOD

Deleted: (REP)

Deleted: lithology

Deleted: taken from observational surveys.

Page 3: [1] Deleted	**Zhang, Zhe**	**8/8/19 9:42:00 AM**
Page 34: [2] Deleted	**Zhang, Zhe**	**8/20/19 2:16:00 PM**
Page 34: [3] Deleted	**Zhang, Zhe**	**8/20/19 2:16:00 PM**
Page 35: [4] Deleted	**Zhang, Zhe**	**8/20/19 2:17:00 PM**